

Covering a set of line segments with a few squares

Joachim Gudmundsson¹, Mees van de Kerkhof², André van Renssen³, Frank Staals⁴,
Lionov Wiratma⁵, and Sampson Wong⁶

¹University of Sydney, Australia, joachim.gudmundsson@sydney.edu.au

²Utrecht University, Netherlands, m.a.vandekerkhof@uu.nl

³University of Sydney, Australia, andre.vanrenssen@sydney.edu.au

⁴Utrecht University, Netherlands, f.staals@uu.nl

⁵Parahyangan Catholic University, Indonesia, lionov@unpar.ac.id

⁶University of Sydney, Australia, swon7907@uni.sydney.edu.au

Abstract

We study three covering problems in the plane. Our original motivation for these problems come from trajectory analysis. The first is to decide whether a given set of line segments can be covered by up to $k = 4$ unit-sized, axis-parallel squares. We give linear time algorithms for $k \leq 3$ and an $O(n \log n)$ time algorithm for $k = 4$.

The second is to build a data structure on a trajectory to efficiently answer whether any query subtrajectory is coverable by up to three unit-sized axis-parallel squares. For $k = 2$ and $k = 3$ we construct data structures of size $O(n\alpha(n) \log n)$ in $O(n\alpha(n) \log n)$ time, so that we can test if an arbitrary subtrajectory can be k -covered in $O(\log n)$ time.

The third problem is to compute a longest subtrajectory of a given trajectory that can be covered by up to two unit-sized axis-parallel squares. We give $O(n2^{\alpha(n)} \log^2 n)$ time algorithms for $k \leq 2$.

1 Introduction

Geometric covering problems are a classic area of research in computational geometry. The traditional *geometric set cover problem* is to decide whether one can place k axis-parallel unit-sized squares (or disks) to cover n given points in the plane. If k is part of the input, the problem is known to be NP-hard [7, 15]. Thus, efficient algorithms are known only for small values of k . For $k = 2$ or 3, there are linear time algorithms [6, 20], and for $k = 4$ or 5, there are $O(n \log n)$ time algorithms [16, 18]. For general k , the $O(n^{\sqrt{k}})$ time algorithm for unit-sized disks [12] can be simplified and extended to unit-sized axis-parallel squares [1].

Motivated by trajectory analysis, we study a line segment variant of the geometric set cover problem where the input is a set of n line segments. Given a set of line segments, we say it is *k-coverable* if there exist k unit-sized axis-parallel squares in the plane so that every line segment is in the union of the k squares (we may write coverable to mean k -coverable when k is clear from the context). The first problem we study in this paper is:

Problem 1. *Decide if a set of line segments is k -coverable, for $k \in O(1)$.*

A key difference in the line segment variant and the point variant is that each segment need not be covered by a single square, as long as each segment is covered by the union of the k squares. See Figure 1.

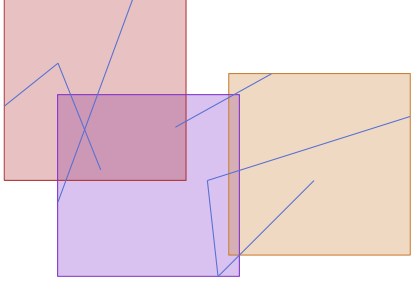


Figure 1: A set of 3-coverable segments.

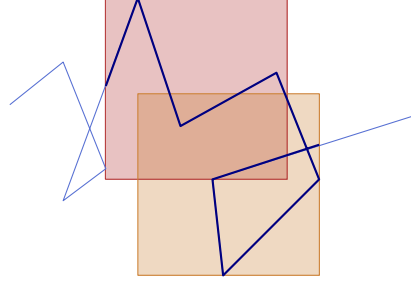


Figure 2: A 2-coverable subtrajectory.

Hoffmann [11] provides a linear time algorithm for $k = 2$ and 3 , however, a proof was not included in his extended abstract. Sadhu et al. [17] provide a linear time algorithm for $k = 2$ using constant space. In Section 2, we provide a proof for a $k = 3$ algorithm and a new $O(n \log n)$ time algorithm for $k = 4$.

Next, we study trajectory coverings. A trajectory \mathcal{T} is a polygonal curve in the plane parametrised by time. Let v_1, \dots, v_n and e_1, \dots, e_{n-1} be the vertices and edges of \mathcal{T} , respectively. For two points s and t on \mathcal{T} , we write $s \prec t$ if s occurs on \mathcal{T} before t . Any such pair of points then defines a unique subtrajectory $\mathcal{T}[s, t]$ of \mathcal{T} starting in s and ending in t . See Figure 2 for an example. Trajectories are commonly used to model the movement of an object (e.g. a bird, a vehicle, etc) through time and space. The analysis of trajectories have applications in animal ecology [5], meteorology [21], and sports analytics [8].

To the best of our knowledge, this paper is the first to study k -coverable trajectories for $k \geq 2$.

A k -coverable trajectory may, for example, model a commonly travelled route, and the squares could model a method of displaying the route (i.e. over multiple pages, or multiple screens), or alternatively, the location of several facilities. We build a data structure that can efficiently decide whether a subtrajectory is k -coverable.

Problem 2. *Construct a data structure on a trajectory, so that given any query subtrajectory, it can efficiently answer whether the subtrajectory is k -coverable, for $k \in O(1)$.*

For $k = 2$ and $k = 3$ we preprocess a trajectory \mathcal{T} with n vertices in $O(n \log n)$ time, and store it in a data structure of size $O(n \log n)$, so that we can test if an arbitrary subtrajectory (not necessarily restricted to vertices) $\mathcal{T}[s, t]$ can be k -covered.

Finally, we consider a natural extension of Problem 2, that is, to calculate the *longest* k -coverable subtrajectory of any given trajectory. This problem is similar in spirit to the problem of covering the maximum number of points by k unit-sized axis-parallel squares [3, 13].

Problem 3. *Given a trajectory, compute a longest k -coverable subtrajectory, for $k \in O(1)$.*

Problem 3 is closely related to computing a trajectory *hotspot*, which is a small region where a moving object spends a large amount of time. For $k = 1$ squares, the existing algorithm by Gudmundsson et al. [9] computes longest 1-coverable subtrajectory of any given trajectory. We notice a missing case in their algorithm, and show how to resolve this issue in the same running time of $O(n \log n)$. Finally, we show how to compute the longest 2-coverable subtrajectory of any given trajectory in $O(n 2^{\alpha(n)} \log^2 n)$ time, where $\alpha(n)$ is the extremely slow growing inverse Ackermann function.

Overview In the next section we consider Problem 1. We build up to the $k = 4$ case by first considering the problem for $k \leq 3$. A simple but crucial observation for $k = 4$ is that if a set S of segments is 4-coverable then either (a) one square has to lie in a corner of the bounding box of S or (b) each square has to touch exactly one side of the bounding box of S . The first case immediately reduces to the case when $k = 3$ which can be solved in linear time, so the focus of Section 2.3 is to solve the second case in $O(n \log n)$ time.

In Section 3 we turn our attention to Problem 2. We build four basic data structures (Tools 1–4) in $O(n\alpha(n) \log n)$ time that are then combined in Sections 3.1 and 3.2 to produce data structures for $k = 2$ and $k = 3$, respectively.

Our main technical contributions are in Sections 4 and 5 where we consider Problem 3 for $k \leq 2$. We first note that an earlier algorithm for $k = 1$ by Gudmundsson et al. [9] omits a possible scenario. We show how this case can be handled in $O(n \log n)$ time before we show our main result for $k = 2$, which is an $O(n2^{\alpha(n)} \log^2 n)$ time algorithm.

2 Problem 1: The Decision Problem

We first consider the simple case when $k = 2$ to build intuition for the problem and state several basic properties that will be used in later sections.

2.1 Is a set of line segments 2-coverable?

We begin with an observation that applies to any k -covering.

Observation 1. *Every k -covering of S must touch all four sides of $\mathcal{BB}(S)$.*

The reasoning behind Observation 1 is simple: if the covering does not touch one of the four sides, say the left side, then the covering could not have covered the leftmost vertex of the set of segments. An intuitive way for two squares to satisfy Observation 1 is to place the two squares in opposite corners of the bounding box. This intuition is formalised in Lemma 1.

Lemma 1 (Sadhu et al. [17]). *A set S of segments is 2-coverable if and only if there is a covering with squares in opposite corners of $\mathcal{BB}(S)$.*

It suffices to check the two configurations where squares are in opposite corners of the bounding box. For each of these two configurations, we simply check if each segment is in the union of the two squares, which takes linear time in total, leading to the following theorem:

Theorem 1. *One can compute a 2-covering of a set of n line segments, or report that no such covering exists, in $O(n)$ time.*

2.2 Is a set of line segments 3-coverable?

The following lemma is analogous to Lemma 1, but for the $k = 3$ case.

Lemma 2. *A set of segments S is 3-coverable if and only if there is a covering with a square in a corner of the bounding box $\mathcal{BB}(S)$.*

Proof. By Observation 1, any 3-covering of S touches all four sides of the bounding box. By the pigeon-hole principle, one of these square must intersect at least two sides of $\mathcal{BB}(S)$.

Consider if these two sides are adjacent. Without loss of generality they are the left and top sides of $\mathcal{BB}(S)$. If the top-left corner of \mathcal{H} already coincides with the top-left corner of $\mathcal{BB}(S)$ the

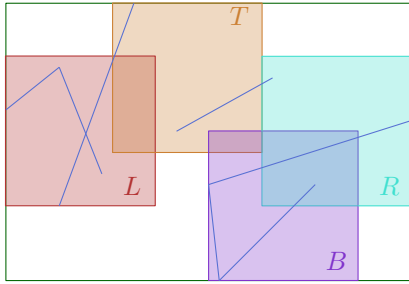


Figure 3: The squares L , T , B and R .

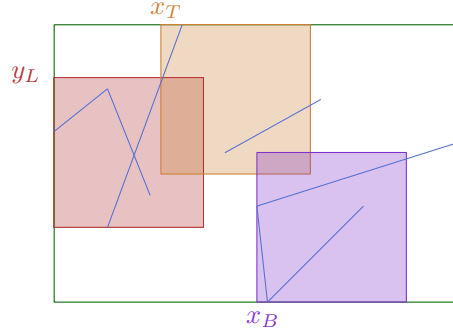


Figure 4: The variables y_L , x_T and x_B .

lemma statement holds. If not, the top-left corner of \mathcal{H} lies outside of $\mathcal{BB}(S)$, and thus we can shift \mathcal{H} to make the two top-left corners coincide.

This increases the area of $\mathcal{BB}(S)$ covered by \mathcal{H} , and hence the 3-covering remains valid.

Consider if these two sides are opposite. Without loss of generality they are the top and bottom sides of $\mathcal{BB}(S)$. Consider the square that intersects the left side of $\mathcal{BB}(S)$ and shift it to coincide with the top-left corner of $\mathcal{BB}(S)$. Since the height of $\mathcal{BB}(S)$ is at most one, we still have a valid 3-covering, and this square intersects three sides of $\mathcal{BB}(S)$. \square

It suffices to consider four cases, one for each corner of the bounding box. After placing the first square in one of the four corners, we subdivide each segment into at most one subsegment that is covered by the first square, and up to two subsegments that are not yet covered. Finally, we use Theorem 1 to decide whether the final two squares can cover all remaining subsegments.

Subdividing each segment takes linear time in total. There are at most a linear number of remaining subsegments. Checking if the remaining segments are 2-coverable takes linear time by Theorem 1. Hence:

Theorem 2. *One can compute a 3-covering of a set of n line segments, or report that no such covering exists, in $O(n)$ time.*

2.3 Is a set of line segments 4-coverable?

By Observation 1, the four squares of a 4-covering must touch all four sides of the bounding box. We have two cases. In the first case, we have a 4-covering with a square in a corner of the bounding box. In the second case, we have a 4-covering with each square touching exactly one side of the bounding box.

In the first case we can use the same strategy as in the three squares case by placing the first square in a corner and then (recursively) checking if three additional squares can cover the remaining subsegments. This gives a linear time algorithm for the first case.

For the remainder of this section, we focus on solving the second case. Define L , B , T , and R to be the square that touches the left, bottom, top and right side of the bounding box of S , respectively. See Figure 3. Without loss of generality, suppose that T is to the left of B . This implies that the left to right order of the squares is L , T , B , R . Suppose for now there was a way to compute the initial placement of L . Then we can deduce the position of T as follows.

Lemma 3. *Given the position of L , if three additional squares can be placed to cover the remaining subsegments, then it can be done with T in the top-left corner of the bounding box of the remaining subsegments.*

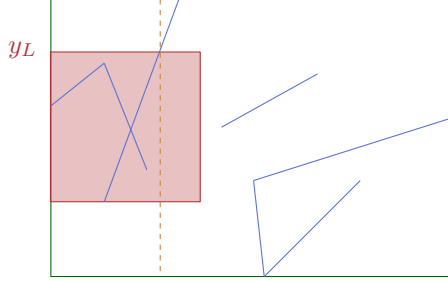


Figure 5: The best position for T is in the top left corner of the bounding box of the remaining subsegments.

Proof. Consider the bounding box of the subsegments not covered by L , in particular, the left side of said bounding box. By definition, there exists a left endpoint of a remaining subsegment that lies on this left side ℓ (the dashed line segment in Figure 5). Suppose that the left side of T is to the right of ℓ : then the squares B and R would be even further right than T , and no square would cover this left endpoint of a remaining subsegment. Hence, if a covering exists, the left side of T cannot be to the right of ℓ .

Suppose that there exists a covering where the left side of T is to the left of ℓ . Then we can shift T so that its left side is aligned with ℓ . As in the proof of Lemma 2 the new position covers more of the area inside the bounding box of the remaining subsegments, and hence we still have a valid covering. Furthermore, since T is also incident to the top-side of $\mathcal{BB}(S)$ (and L is not incident to $\mathcal{BB}(S)$) it follows that the top-left corner of T now coincides with the top-side of the bounding box of the remaining subsegments as desired. \square

After placing the first two squares, we can place B in the bottom-left corner of the bounding box of the remaining segments, for reasons analogous to Lemma 3. Finally, we cover the remaining segments with R , if possible.

It follows that the position of L along the left boundary uniquely determines the positions of the squares T , B and R along their respective boundaries. Unfortunately, we do not know the position of L in advance, so instead we consider all possible initial positions of L via parametrisation. Let y_L be the y -coordinate of the top side of L , and similarly let x_T , x_B be the x -coordinates of the left side of T and B , respectively. See Figure 4.

Finally, we will try to cover all remaining subsegments with the square R . Define x_{R_1} and x_{R_2} to be the x -coordinates of the leftmost and rightmost uncovered points after the first three squares have been placed. Similarly, define y_{R_1} and y_{R_2} to be the y -coordinates of the topmost and bottommost uncovered points. Then it is possible to cover the remaining segments with R if and only if $x_{R_1} - x_{R_2} \leq 1$ and $y_{R_1} - y_{R_2} \leq 1$.

Since the position of L uniquely determines T , B and R , we can deduce that the variables x_T , x_B , x_{R_1} , x_{R_2} , y_{R_1} and y_{R_2} are all functions of y_L . We will show that each of these functions is piecewise linear and can be computed in $O(n \log n)$ time. We begin by computing x_T as a function of variable y_L .

Let $s \in S$ be a segment, we define $f_s(y) = \min_{p \in s \wedge p_y \geq y} p_x$ as the leftmost point on s above the horizontal line at height y , and $f(y) = \min_{s \in S} f_s(y)$ as the minimum over all segments s . We refer to (the graph of) f as the *skyline* of S .

Lemma 4. *The skyline f of a set S of n segments is a piecewise linear, monotonically increasing function with $O(n\alpha(n))$ pieces and can be computed in $O(n \log n)$ time, where $\alpha(n)$ is the inverse*

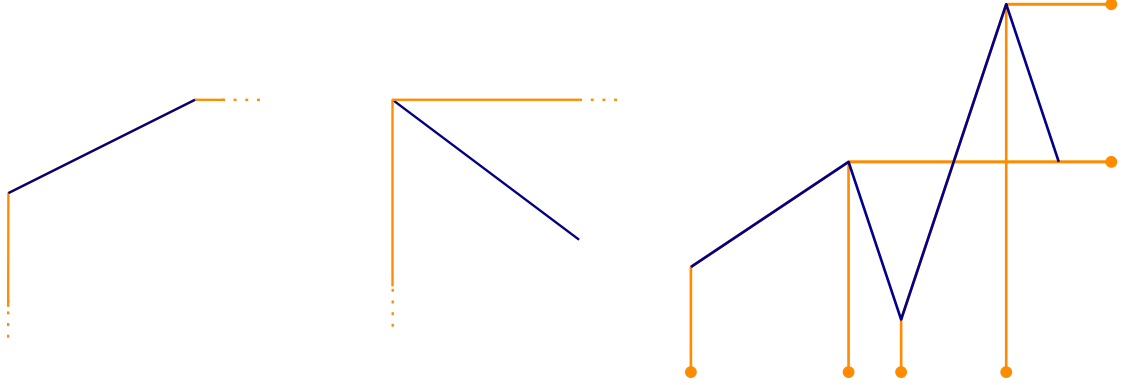


Figure 6: The skyline of a segment with positive gradient (left), a segment with negative gradient (middle) and a set of segments (right).

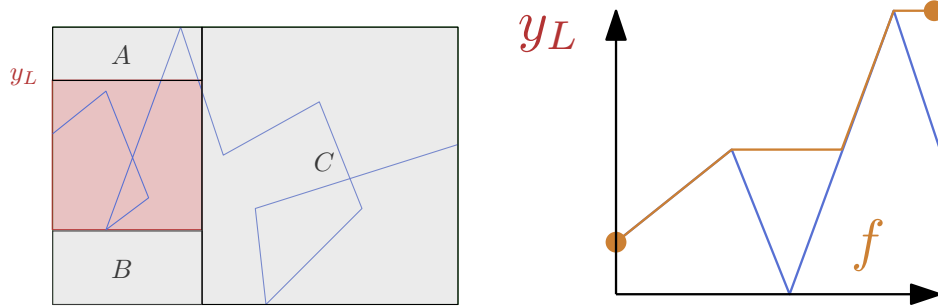


Figure 7: The regions A , B and C are above, below, and to the left of the square L (left). The skyline is the leftmost point of region A as y_L increases (right).

Ackermann function.

Proof. We first compute the skyline of each individual segments. If the segment has positive gradient, then the skyline consists of three pieces. If the segment has negative gradient, then the skyline has two pieces. See Figure 6, (left) and (middle). Next, we merge the individual skylines into a combined skyline. For any ℓ , the function $f(\ell)$ takes the value of the leftmost intersection of the individual skylines with ℓ , i.e. the upper envelope except in the leftwards cardinal direction rather than the upwards direction. See Figure 6, (right).

The skylines of individual segments can be computed in $O(n)$ time, and have a total size of $O(n)$. The leftwards envelope of the individual skylines has at most $O(n\alpha(n))$ pieces and can be computed in $O(n \log n)$ time [19]. The leftwards envelope is piecewise linear and a monotonically increasing function. \square

Now we can apply Lemma 4 to compute x_T as a function of y_L .

Lemma 5. *The variable x_T as a function of variable y_L is a piecewise linear, monotonically increasing function of complexity $O(n\alpha(n))$ and can be computed in $O(n \log n)$ time.*

Proof. We divide the region inside the bounding box and not covered by L into three subregions. The region A is above L , the region B is below L and the region C is to the right of L . See

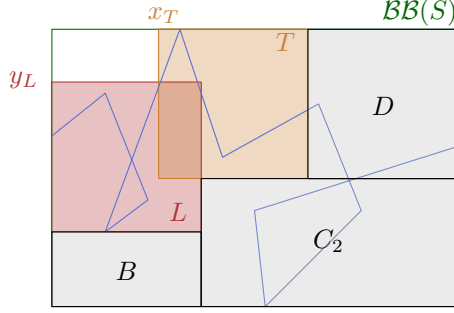


Figure 8: The regions B , D and C_2 as defined by L and T .

Figure 7 (left). As y_L increases, the leftmost point of A follows the skyline of the segments in A . See Figure 7, (right). Analogously, as y_L increases, the leftmost point of B follows the skyline of the segments in B , except that the skyline is taken in the downward direction instead. Finally, as y_L increases, the leftmost point of C is a constant. By Lemma 4, the leftmost points of A , B and C are all piecewise linear functions with complexities $O(n\alpha(n))$ that can be computed in $O(n \log n)$ time. The value of x_T is the minimum of these functions, so is a piecewise linear function of complexity $O(n\alpha(n))$ and can be computed in $O(n \log n)$ time. \square

Next, we show that x_B is a piecewise linear function of y_L , with complexity $O(n\alpha(n))$, and can be computed in $O(n \log n)$ time.

Lemma 6. *The variable x_B as a function of variable y_L is a piecewise linear function of complexity $O(n\alpha(n))$ and can be computed in $O(n \log n)$ time.*

Proof. For an analogous reason to Lemma 3, we can place B in the bottom-right corner of the remaining segments after placing L and T . Therefore, x_B is the x -coordinate of the leftmost uncovered point after placing L and T . Divide the remaining region into three subregions: B below L , D to the right of T , and C_2 to the right of L and below T . See Figure 8.

As y_L increases, the leftmost point of B moves monotonically to the left, and follows the skyline of the set of segments, except that the skyline is taken in the downwards direction. By Lemma 4, the leftmost point of B is a piecewise linear function in terms of y_L and can be computed in $O(n \log n)$ time.

As y_L increases, the position of square T , given by the variable x_T moves monotonically to the right, and follows a skyline of the segments. We have shown in Lemma 5 that x_T is a piecewise linear function in terms of y_L and can be computed in $O(n \log n)$ time. Similarly, the leftmost point of D is a piecewise linear function in terms of the position of T and can be computed in $O(n \log n)$ time. We compose the leftmost point of D as a piecewise linear function of x_T , and x_T as a piecewise linear function of y_L . By Lemma 4, each of these functions are monotonically increasing functions with complexity $O(n\alpha(n))$. Composing two monotonic, piecewise linear functions requires a single simultaneous sweep of the two functions, which takes $O(n\alpha(n))$ time. Hence, the leftmost point of D is a piecewise linear function and can be computed in $O(n \log n)$ time.

As y_L increases, the region C_2 remains constant, so the leftmost point of C_2 remains constant. This point can be computed in $O(n)$ time.

Putting this all together, each of the leftmost points of B , D and C_2 are piecewise linear functions in terms of y_L and can be computed in $O(n \log n)$ time. Hence, their minimum x_B is a piecewise linear function of complexity $O(n\alpha(n))$ and can be computed in $O(n \log n)$ time. \square

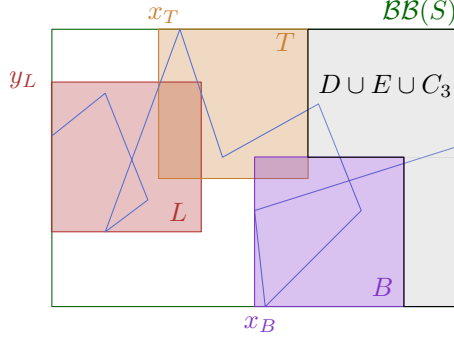


Figure 9: The regions $D \cup E \cup C_3$ as defined by L , T and B .

Then we compute x_{R_1} , x_{R_2} , y_{R_1} and y_{R_2} in a similar fashion.

Lemma 7. *The variables x_{R_1} , x_{R_2} , y_{R_1} , y_{R_2} as functions of variable y_L are piecewise linear functions of complexity $O(n\alpha(n))$ and can be computed in $O(n \log n)$ time.*

Proof. We will show that y_{R_1} as a function of y_L is a piecewise linear function and can be computed in $O(n \log n)$ time. The other variables follow analogously.

Divide the region to the right of L , T and B into three subregions: D is to the right of L and above B , E to the right of B , and C_3 below D and above B , if it exists. Note that C_3 only exists in squares where the height of the bounding box is greater than two. Otherwise, only the regions D and E exist, as shown in Figure 9. We compute the topmost points of D , E and C_3 separately, then return their overall topmost point to be the value of y_{R_1} .

As y_L increases, the position of square T given by the variable x_T moves monotonically to the right and follows the skyline of the segments. Similarly, as x_T moves monotonically to the right, the topmost point of D moves monotonically to the right. We have shown that each of these monotonic functions are piecewise linear, have complexity $O(n\alpha(n))$ and can be computed in $O(n \log n)$ time (See Lemma 4). Computing their composition of monotonic, piecewise linear functions requires a single simultaneous sweep of the two functions, which takes $O(n\alpha(n))$. Hence, the overall function is piecewise linear and can be computed in $O(n \log n)$.

As y_L increases, the topmost point of E is similarly a composition of two skyline functions, which is piecewise linear and can be computed in $O(n \log n)$.

Finally, as y_L increases, the topmost point of C_3 (if it exists) is constant and can be computed in $O(n)$ time.

Putting this all together, each of the leftmost points of D , E and C_3 are piecewise linear functions in terms of y_L and can be computed in $O(n \log n)$ time. Hence, their minimum y_{R_1} is a piecewise linear function of complexity $O(n\alpha(n))$ and can be computed in $O(n \log n)$ time. \square

Finally, we check if there exists a value of y_L so that $x_{R_1} - x_{R_2} \leq 1$ and $y_{R_1} - y_{R_2} \leq 1$. If so, there exist positions for L , B , T and R that cover all the segments, otherwise, there is no such position. This yields the following result:

Theorem 3. *One can decide if a set of n segments is 4-coverable in $O(n \log n)$ time.*

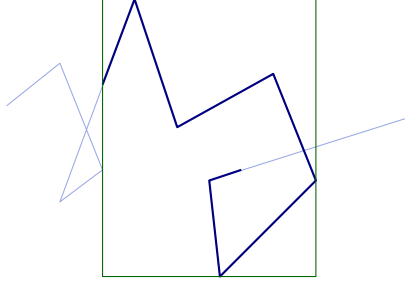


Figure 10: The subtrajectory data structure that returns the bounding box.

3 Problem 2: The Subtrajectory Data Structure Problem

Let \mathcal{T} be a piecewise linear trajectory of complexity n . We briefly describe some tools, then we use our tools to construct data structures for answering if a subtrajectory is either 2-coverable or 3-coverable.

Tool 1. A linear size “bounding box” data structure that can be built in $O(n)$ time and given a pair of query points $s \prec t$ on \mathcal{T} can return the bounding box of $\mathcal{T}[s, t]$ in $O(\log n)$ time.

Proof. Construct a binary tree on the sequence of edges in \mathcal{T} . For each node in the binary tree, the segments that are its descendants form a contiguous subtrajectory of \mathcal{T} . We call such a contiguous subtrajectory a canonical subset. For each internal node, we compute the bounding box of its canonical subset. If we compute the bounding boxes in a bottom up fashion, each internal node can be processed in constant time. The overall construction time is $O(n)$.

Given a query subtrajectory, we decompose the subtrajectory into canonical subsets. We query the data structure to obtain an individual bounding box for each canonical subset. We compute a combined bounding box that contains all individual bounding boxes. The overall query time is $O(\log n)$. \square

Tool 2. An $O(n\alpha(n)\log n)$ size “upper envelope” data structure that can be built in $O(n\alpha(n)\log n)$ time and given a pair of query points $s \prec t$ on \mathcal{T} and a vertical line can return the highest intersection between the line and subtrajectory $\mathcal{T}[s, t]$ (if one exists) in $O(\log n)$ time. See Figure 11.

Proof. We use an approach similar to Tool 1. We build a binary search tree over segments of \mathcal{T} , and associate with each internal node the subset of all its descendants. We call this the canonical subset associated with this internal node. By construction, every subtrajectory can be decomposed into a union of $O(\log n)$ canonical subsets.

At each internal node, we store the upper envelope of all segments in its canonical subset. This upper envelope can be represented by an list of its vertices in left-to-right order. Since the upper envelope of n line segments has size $O(n\alpha(n))$, the total size of our data structure is $O(n\alpha(n)\log n)$. Computing all these upper envelopes can be done in $O(n\alpha(n)\log n)$ time using a bottom up divide and conquer approach [10].

Given a query subtrajectory and a vertical line at x -coordinate x , we can naively answer the upper envelope query in two steps. First, we decompose the subtrajectory into $O(\log n)$ canonical subsets, and find the segment realizing the upper envelope at x using a binary search in $O(\log(n\alpha(n))) = O(\log n)$ time. Second, we report the highest intersection point of the vertical line

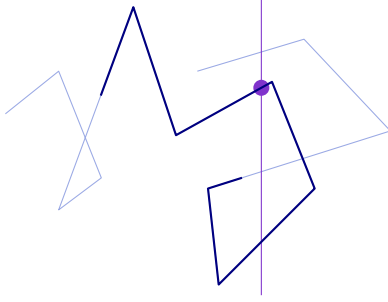


Figure 11: Tool 2 returns the highest intersection of a subtrajectory and a vertical line.

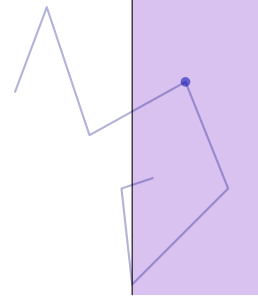


Figure 12: Tool 3 returns the highest subtrajectory vertex in a query slab.

with the $O(\log n)$ segments found. The overall query time for this approach would be $O(\log^2 n)$ time. A standard application of fractional cascading [4] reduces the total query time to $O(\log n)$. \square

Using Tool 2 we can report whether a vertical half-line intersects a subtrajectory. We build Tool 2 in all four cardinal directions. Similarly, we will build Tool 3 and Tool 4 in all four cardinal directions.

Tool 3. An $O(n \log n)$ size “highest vertex” data structure that can be built in $O(n \log n)$ time and given a pair of query points $s \prec t$ on \mathcal{T} and a vertical query slab can return the highest vertex of \mathcal{T} in subtrajectory $\mathcal{T}[s, t]$ in the slab in $O(\log n)$ time. See Figure 12.

Proof. We store \mathcal{T} in the leaves of a balanced binary search tree in order along the trajectory. For each internal node ν , corresponding to a canonical subset of vertices \mathcal{T}_ν , we store this set of points ordered on increasing x -coordinate. In addition, we store their y -coordinates in an array A_ν in this order. That is, $A_\nu[i]$ stores the y -coordinate of the point p_i with the i^{th} -largest x -coordinate among \mathcal{T}_ν . Each entry in the sequence \mathcal{T}_ν will store its index in A_ν , moreover we assume that for each index i we can again retrieve the point p_i (e.g. by storing another array that stores the original points). We preprocess A_ν for constant time range maximum queries [2], and we build a fractional cascading structure on canonical subsets \mathcal{T}_ν [4]. Since each node uses linear space, the total space required is $O(n \log n)$. Moreover, by building the sorted lists \mathcal{T}_ν in a bottom-up fashion we can build the entire data structure in $O(n \log n)$ time as well.

To answer a query, we find the $O(\log n)$ nodes whose canonical subsets make up the query subtrajectory. For each such node ν , the points from \mathcal{T}_ν that lie in the query slab are stored consecutively in \mathcal{T}_ν (and A_ν). So, using the fractional cascading structure we can find, the index i_ν of the leftmost point among \mathcal{T}_ν that lies in the vertical query slab. This takes $O(\log n)$ time in total. Similarly, we get the index j_ν of the rightmost point from \mathcal{T}_ν in the query slab. We can then query the range maximum structure on the array A_ν with the range i_ν, \dots, j_ν to find the point with maximum y -coordinate in constant time. We do this for all $O(\log n)$ nodes and report the highest point found. It follows that this is the highest vertex on the query subtrajectory that also lies in the query slab. \square

Tool 4. An $O(n \log n)$ size “highest vertex” data structure that can be built in $O(n \log n)$ time and given a pair of query points $s \prec t$ on \mathcal{T} and a query quadrant $Q = [Q_x, \infty) \times [Q_y, \infty)$ can return the highest vertex of \mathcal{T} in $\mathcal{T}[s, t] \cap Q$ in $O(\log n)$ time.

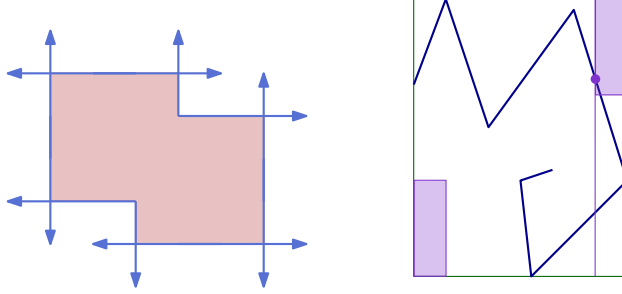


Figure 13: The union of two squares and the half-lines that do not intersect the interior (left). One of the four half-lines on the boundary of the union of two squares (right).

Proof. We again store the vertices of \mathcal{T} in the leaves of a balanced binary search tree in order along the trajectory. For each internal node ν , consider the function $f_\nu(x)$ expressing the maximum y -coordinate among the points in T_ν right of the vertical line at x . Observe that this function is piecewise constant, monotonically decreasing, and has complexity $O(n)$. We store the graph of this function f_ν by storing an ordered sequence of its breakpoints, which allows us to evaluate $f_\nu(x)$ for some value x in $O(\log n)$ time by a binary search. The data structure uses $O(n \log n)$ space, and can be built in $O(n \log n)$ time (e.g. again by sorting the points on increasing x -coordinate in a bottom up fashion).

To answer a query, we find the $O(\log n)$ nodes whose canonical subsets make up the query subtrajectory. For each such node ν , we evaluate $f_\nu(Q_x)$, and compute the maximum over all nodes. If this value is at least Q_y the corresponding point is the highest vertex of the query subtrajectory in quadrant Q , and hence we can report it. If the value is smaller than Q_y the quadrant is empty. The query time is $O(\log^2 n)$ time, which we can reduce to $O(\log n)$ using fractional cascading [4]. \square

Using a data structure analogous to Tool 4 we can also report the lowest point on the query subtrajectory in a quadrant $[Q_x, \infty) \times [Q_y, \infty)$.

3.1 Query if a subtrajectory is 2-coverable

We start with a lemma to help us apply Tool 2 to the boundary of the union of two axis aligned unit squares.

Lemma 8. *The union $\mathcal{U} = \mathcal{H}_1 \cup \mathcal{H}_2$ be of two axis aligned unit squares has constant complexity, every edge \overline{uv} of \mathcal{U} is axis aligned, and at least one of the half-lines \overrightarrow{uv} and \overrightarrow{vu} does not intersect the interior of \mathcal{U} . See Figure 13, (left).*

Proof. The only non-trivial part of the Lemma is to argue that for every edge \overline{uv} either \overrightarrow{uv} or \overrightarrow{vu} does not intersect the interior of \mathcal{U} . Assume w.l.o.g. that \overline{uv} is part of the boundary of \mathcal{H}_1 (and thus lies outside of \mathcal{H}_2), and assume that \overrightarrow{uv} intersects the interior of \mathcal{U} (otherwise the claim already holds). It follows that \overrightarrow{uv} intersects the interior of \mathcal{H}_2 . By convexity of \mathcal{H}_2 it then follows \overrightarrow{vu} does not intersect the interior of \mathcal{H}_2 , otherwise \overline{uv} would be contained in \mathcal{H}_2 . This completes the proof. \square

Now we are ready to prove the main result of Section 3.1.

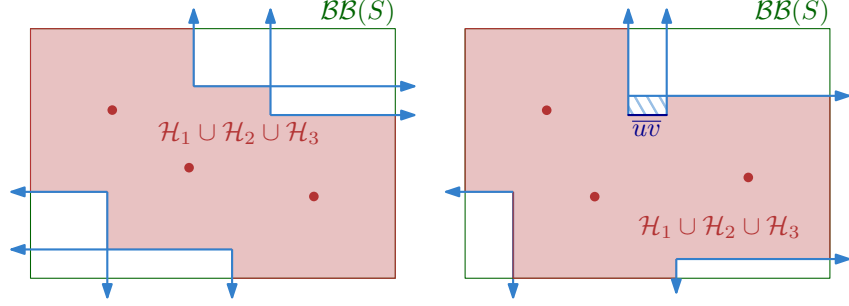


Figure 14: The boundary pieces of the union and the cardinal directions we can extend the boundary piece indefinitely.

Theorem 4. *Let \mathcal{T} be a trajectory with n vertices. After $O(n\alpha(n) \log n)$ preprocessing time, \mathcal{T} can be stored using $O(n\alpha(n) \log n)$ space, so that deciding if a query subtrajectory $\mathcal{T}[a, b]$ is 2-coverable takes $O(\log n)$ time.*

Proof. Our construction procedure is to build Tool 1, and Tool 2 for all four cardinal directions. Our query procedure consists of three steps. First, we use Tool 1 to compute the bounding box of the subtrajectory. Second, we apply Lemma 1 to obtain a configuration of two squares. Finally, we check if the subtrajectory is inside the union of the two squares. We do so by using Tool 2 to check if the subtrajectory passes through any of the four half-lines on the boundary of the union, see Figure 13, (right). The construction procedure takes $O(n\alpha(n) \log n)$ time and space. The query procedure takes $O(\log n)$ time. \square

3.2 Query if a subtrajectory is 3-coverable

We start with a lemma analogous to Lemma 8, but for three squares.

Lemma 9. *The union $\mathcal{U} = \mathcal{H}_1 \cup \mathcal{H}_2 \cup \mathcal{H}_3$ be of three axis aligned unit squares has constant complexity, every edge \overline{uv} of \mathcal{U} is axis aligned, and there is at most one edge \overline{uv} for which both the half-lines \overrightarrow{uv} and \overrightarrow{vu} both intersect the interior of \mathcal{U} . See Figure 14.*

Proof. Assume, by contradiction, that there are two edges $\overline{u_1v_1}$ and $\overline{u_2v_2}$ for which both rays intersect the interior of \mathcal{U} .

Assume without loss of generality that $\overline{u_2v_2}$ lies on the top side of \mathcal{H}_2 (otherwise rotate the plane), and that u_2 lies left of v_2 . Since the squares are all convex, it now follows that: (i) $\overrightarrow{u_2v_2}$ and $\overrightarrow{v_2u_2}$ do not intersect the interior of \mathcal{H}_2 , and (ii) that they cannot both intersect the same \mathcal{H}_i . So, assume without loss of generality that $\overrightarrow{u_2v_2}$ intersects \mathcal{H}_3 and that $\overrightarrow{v_2u_2}$ intersects \mathcal{H}_1 . It then follows that the left to right ordering of (the centers of) the squares is $\mathcal{H}_1, \mathcal{H}_2, \mathcal{H}_3$. Furthermore, (the center of) \mathcal{H}_2 is the lowest center among the three squares.

We now argue that $\overline{u_1v_1}$ cannot also be horizontal. Via the same reasoning as above, $\overrightarrow{u_1v_1}$ and $\overrightarrow{v_1u_1}$ must hit different squares, and thus $\overline{u_1v_1}$ must lie on the middle square \mathcal{H}_2 . In particular, since \mathcal{H}_2 is the lowest square and the squares have the same size, $\overline{v_1u_1}$, it must lie on the top side of \mathcal{H}_2 as well (the horizontal line through the bottom side does not intersect \mathcal{H}_1 or \mathcal{H}_3). That implies that two oppositely oriented rays (e.g. $\overrightarrow{u_2v_2}$ and $\overrightarrow{v_1u_1}$) intersect the same square (e.g. \mathcal{H}_3). However, since all squares have the same size we again get a contradiction.

So $\overline{u_1v_1}$ is vertical, with say u_1 below v_1 . We once again have that $\overrightarrow{u_1v_1}$ and $\overrightarrow{v_1u_1}$ must intersect different squares. Moreover, the centers of these squares must lie on the same of the vertical line

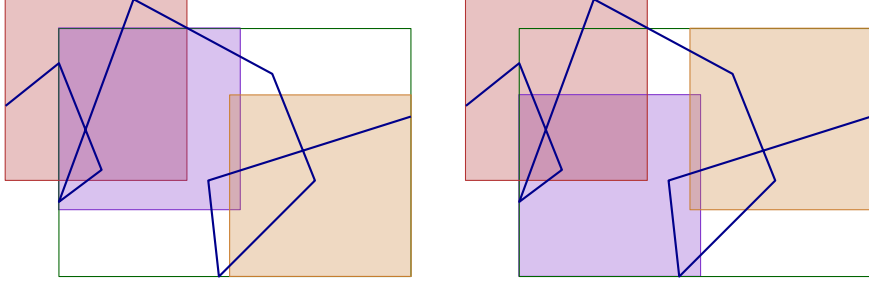


Figure 15: The second and third squares in one of two configurations.

through $\overline{u_1v_1}$. Consider the case that these centers lie right of this line. The other case is symmetric. It now follows that $\overline{u_1v_1}$ must lie on the leftmost square \mathcal{H}_1 , and that the square below $\overline{u_1v_1}$ must be \mathcal{H}_2 . More specifically, u_1 must lie on or above the top side of \mathcal{H}_2 (again since the squares have the same size). Similarly, v_1 must lie below the bottom side of \mathcal{H}_3 . However, this implies that the bottom side of \mathcal{H}_3 lies above the top side of \mathcal{H}_2 , and thus the horizontal ray $\overrightarrow{u_2v_2}$ does not intersect the interior of \mathcal{H}_3 . Contradiction. \square

Now we can prove the main result of Section 3.2.

Theorem 5. *Let \mathcal{T} be a trajectory with n vertices. After $O(n\alpha(n)\log n)$ preprocessing time, \mathcal{T} can be stored using $O(n\alpha(n)\log n)$ space, so that deciding if a query subtrajectory $\mathcal{T}[a, b]$ is 3-coverable takes $O(\log n)$ time.*

Proof. Our construction procedure is to build Tool 1, and Tools 2, 3, and 4 in all four cardinal directions. The total preprocessing time and space usage is $O(n\alpha(n)\log n)$.

Our query procedure consists of three steps. The first step is to place the first square in the corner of the bounding box. The second step is to place the second and third squares in one of two configurations, see Figure 15. The third step is to check if the configuration of three squares covers the subtrajectory.

In the first step, we use Tool 1 to compute the bounding box of the query subtrajectory, and then apply Lemma 2 to place the first square in a corner of the bounding box.

In the second step, we compute the bounding box of the uncovered segments after placing the first box. Then we apply Lemma 1 to place the final two squares in opposite corners of the bounding box of the uncovered subsegments. See Figure 15. Suppose we placed a square in the top-left corner in the first step. We have two cases for the topmost uncovered point: it is either a vertex of the subtrajectory, or the intersection of a subtrajectory edge with the left or bottom side of the top-left square. The first case can be handled by two queries to Tool 4. The second case can be handled by querying Tool 2 along the right or bottom boundaries of the top-left square, and taking the highest of these points. We apply the same procedure in all four cardinal directions to obtain the bounding box of the uncovered subsegments, as required.

For the third step, we check if a given configuration $\mathcal{U} = \mathcal{H}_1 \cup \mathcal{H}_2 \cup \mathcal{H}_3$ of three squares covers the subtrajectory $\mathcal{T}[a, b]$. The approach is similar to the two square case: we check if the starting point a lies inside \mathcal{U} , and if the subtrajectory ever exits \mathcal{U} . We use a combination of Tools 2, 3 and 4, to achieve this.

By Lemma 9 there is at most one edge \overline{uv} on the boundary of \mathcal{U} for which both rays \overrightarrow{uv} and \overrightarrow{vu} hit the (interior of) \mathcal{U} . Hence, for all edges other than \overline{uv} we can check if the subtrajectory exits \mathcal{U} using an appropriate copy of Tool 2. Observe that if the subtrajectory does not intersect the

boundary of \mathcal{U} in any edge other than \overline{uv} then either it exits \mathcal{U} through \overline{uv} and does not return, or it exits and reenters \mathcal{U} through \overline{uv} . In both cases a vertex of $\mathcal{T}[a, b]$ (possibly its endpoint) must lie in the connected component of $\mathcal{BB}(\mathcal{T}[a, b]) \setminus \mathcal{U}$ that is incident to \overline{uv} . We can check this using Tools 3 and 4.

All in all we make a constant number of queries to Tools 1, 2, 3, and 4, each of which takes $O(\log n)$ time. Hence, we can test if a query subtrajectory is 3-coverable in $O(\log n)$ time. \square

4 Problem 3 for $k = 1$: A Longest 1-Coverable Subtrajectory

In this section we compute a longest k -coverable subtrajectory $\mathcal{T}[p^*, q^*]$ of a given trajectory \mathcal{T} for $k = 1$. Note that the start and end points p^* and q^* of such a subtrajectory need not be vertices of the original trajectory. Gudmundsson, van Kreveld, and Staals [9] presented an $O(n \log n)$ time algorithm for the case $k = 1$. However, we note that there is a mistake in one of their proofs, and hence their algorithm misses one of the possible scenarios. We show how this case can also be handled in $O(n \log n)$ time, thus correcting their mistake.

Gudmundsson, van Kreveld, and Staals state that there exists an optimal placement of a unit square, i.e. one such that the square covers a longest 1-coverable subtrajectory of \mathcal{T} , and has a vertex of \mathcal{T} on its boundary [9, Lemma 7]. However, that is incorrect, as illustrated in Figure 16. Let $p(t)$ be a parametrisation of the trajectory. Fix a corner c of the square and shift the square so that c follows $p(t)$. Let $q(t)$ be the point so that $\mathcal{T}[p(t), q(t)]$ is the maximal subtrajectory contained in the square, and let $\phi(t)$ be the length of this subtrajectory. This function ϕ is piecewise linear, with inflection points not only when a vertex of \mathcal{T} lies on the boundary of the square, but also when $p(t)$ or $q(t)$ hits a corner of the square. The argument in [9] misses this last case. Instead, the correct characterization is:

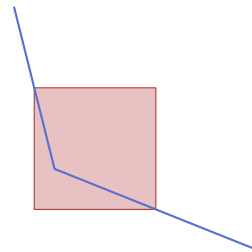


Figure 16: An optimal placement that has no vertex on the boundary of the square.

Lemma 10. *Given a trajectory \mathcal{T} with vertices v_1, \dots, v_n , there exists a square \mathcal{H} covering a longest 1-coverable subtrajectory so that either:*

- *there is a vertex v_i of \mathcal{T} on the boundary of \mathcal{H} , or*
- *there are two trajectory edges passing through opposite corners of \mathcal{H} .*

Proof. Proof by contradiction. Assume that \mathcal{H}^* is an optimal square (i.e. covering a longest 1-coverable subtrajectory), and there is no optimal square satisfying the conditions in the lemma statement. Since \mathcal{H}^* is optimal, the longest contiguous subtrajectory $\mathcal{T}^* = \mathcal{T}[p^*, q^*]$ in \mathcal{H}^* must touch two opposite sides of \mathcal{H}^* . Assume without loss of generality that these sides are horizontal.

Let $\mathcal{H}' = \mathcal{H}^*$ and let \mathcal{T}' be a maximal length sub-trajectory in \mathcal{H}' , such that initially $\mathcal{T}' = \mathcal{T}^*$. It is easy to see that we can shift \mathcal{H}' horizontally—while keeping \mathcal{T}^* inside it—until either a vertex of \mathcal{T}' lies on (a vertical side of) $\partial\mathcal{H}'$ or p^* lies on a corner of \mathcal{H}' . In the former case we immediately obtain a contradiction. In the latter case, translate \mathcal{H}' while keeping the starting point p' of \mathcal{T}' on the same corner of \mathcal{H}' (moving the starting point of \mathcal{T}' earlier or later). Let $\phi(t)$ denote the length of \mathcal{T}' as a function of the starting time $t = t_{p'}$ of \mathcal{T}' . Function ϕ has break points when: (i) p' or q' crosses a vertex, (ii) \mathcal{H}' gets a vertex of \mathcal{T}' on its boundary, or (iii) when the side of \mathcal{H}' containing q changes. Since ϕ is (piecewise) linear, we can either increase or decrease t without decreasing $\phi(t)$ until ϕ is at a break point. At such a break point \mathcal{H}' has a vertex of \mathcal{T}' on its

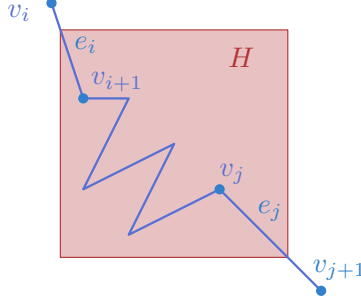


Figure 17: An optimal hotspot H .

boundary (cases (i) and (ii)) or q lies in a corner of \mathcal{H}' (case (iii)). In the former case we arrive at a contradiction. In the latter case, observe that p also lies in a corner of \mathcal{H}' (by definition of ϕ). If this corner is opposite to that of q we satisfy the second condition of the lemma, and thus arrive at a contradiction as well. Otherwise, the two corners lie on the same side, say the top side, of \mathcal{H}' , and thus we can shift \mathcal{H}' upwards while covering \mathcal{T}' , until a vertex of \mathcal{T}' now lies on the bottom side of \mathcal{H}' . Hence, we also arrive at a contradiction in this final case. This completes the proof. \square

To compute a longest 1-coverable subtrajectory we now have two cases, as described by Lemma 10. In the first case, i.e. when there is a vertex v_i on the boundary of H , we use the existing algorithm of Gudmundsson et al. [9] to compute the longest 1-coverable subtrajectory. It remains to handle the second case, i.e. when there are two trajectory edges passing through opposite corners of H . We begin by showing a useful lemma.

Lemma 11. *Given a pair of non-parallel edges e_i and e_j of \mathcal{T} , there is at most one unit square H such that the top left corner of H lies on e_i , and the bottom right corner of H lies on e_j .*

Proof. Let p be the top-left corner of H and q be the bottom right corner of H . Consider as p moves along the edge e_i . Then q also moves along a straight segment, e'_i , that is a translated copy of e_i . By the conditions of the lemma, q also lies on e_j . Therefore, q must be the intersection of e'_i and e_j , if one exists, and the observation follows. \square

It follows that any pair of edges e_i, e_j of \mathcal{T} generates at most a constant number of additional candidate placements that we have to consider. Let \mathcal{H}_{ij} denote this set. Next, we argue that there are only $O(n)$ relevant pairs of edges that we have to consider.

We define the *reach* of a vertex v_i , denoted $r(v_i)$, as the vertex v_j such that $\mathcal{T}[v_i, v_j]$ can be 1-covered, but $\mathcal{T}[v_i, v_{j+1}]$ cannot. Let $\mathcal{H}_i = \mathcal{H}_{(i-1)j}$ denote the set of candidate placements corresponding to v_i and $v_j = r(v_i)$. Analogously, we define the *reverse reach* $rr(v_j)$ of v_j as the vertex v_i such that $\mathcal{T}[v_i, v_j]$ can be 1-covered, but $\mathcal{T}[v_{i-1}, v_j]$ cannot, and the set $\mathcal{H}'_j = \mathcal{H}_{(i-1)j}$. Finally, let $\mathcal{H} = \bigcup_{i=1}^n \mathcal{H}_i \cup \mathcal{H}'_i$ be the set of placements contributed by all reach and reverse reach pairs. By Lemma 12, H_i consists of at most one element. Similarly, H'_i consists of at most one element. Therefore, H is the union of $2n$ sets, each with at most one element, so $|H| = O(n)$.

Lemma 12. *Let $p^* \in e_i$ and $q^* \in e_j$ lie on edges of \mathcal{T} , and let H be a unit square with p^* in one corner, and q^* in the opposite corner. We have that $H \in \mathcal{H}$.*

Proof. Observe that vertices v_{i+1} and v_j are inside H whereas v_i and v_{j+1} are outside of H . See Figure 17. We now distinguish between two cases, depending on whether v_j is reachable from v_i or not.

If v_j is reachable from v_i then v_{j+1} is not (otherwise $\mathcal{T}[v_i, v_{j+1}] \supset \mathcal{T}[p^*, q^*]$ is 1-coverable, and thus $\mathcal{T}[p^*, q^*]$ is not a longest 1-coverable subtrajectory). Hence, $v_j = r(v_i)$ is the reach of v_i , and thus $H \in \mathcal{H}_i \subseteq \mathcal{H}$.

If v_j is not reachable from v_i , then $\mathcal{T}[v_i, v_j]$ cannot be 1-covered. However, since v_{i+1} and v_j are contained in H the subtrajectory $\mathcal{T}[v_{i+1}, v_j]$ can be 1-covered. It follows that v_{i+1} is the reverse reach of v_j , and thus $H \in \mathcal{H}'_j \subseteq \mathcal{H}$. \square

Once we have the reach $r(v_i)$ and the reverse reach $rr(v_i)$ for every vertex v_i we can easily construct \mathcal{H} in linear time (given a pair of edges e_i, e_j we can construct the unit squares for which one corner lies on e_i and the opposite corner lies on e_j in constant time). We can use Tool 1 to test each candidate in $O(\log n)$ time. So all that remains is to compute the reach of every vertex of \mathcal{T} ; computing the reverse reach is analogous.

Lemma 13. *We can compute $r(v_i)$, for each vertex $v_i \in \mathcal{T}$, in $O(n \log n)$ time in total.*

Proof. We can prove this result using a sliding window approach. For v_1 we just naively test the subtrajectories $\mathcal{T}[v_1, v_j]$, starting with $j = 1$ until we find a $\mathcal{T}[v_1, v_{j+1}]$ that we can no longer cover. Hence $r(v_1) = v_j$. To compute the reach of v_{i+1} , we now simply continue this procedure starting with $v_j = r(v_i)$. In total this requires $O(n)$ calls to Tool 1, which take $O(\log n)$ time each. This proves the result. \square

Lemma 13 gives the following result.

Theorem 6. *Given a trajectory \mathcal{T} with n vertices, there is an $O(n \log n)$ time algorithm to compute a longest 1-coverable subtrajectory of \mathcal{T} .*

5 Problem 3 for $k = 2$: A Longest 2-Coverable Subtrajectory

In this section we reuse some of the observations from Section 4 to develop an $O(n2^{\alpha(n)} \log^2 n)$ time algorithm to compute a longest k -coverable subtrajectory for $k = 2$. In particular, we will compute the first such longest 2-coverable subtrajectory $\mathcal{T}[p^*, q^*]$ of \mathcal{T} , and the squares \mathcal{H}_1 and \mathcal{H}_2 that cover $\mathcal{T}[p^*, q^*]$ (and such that $p^* \in \mathcal{H}_1$). We refer to $\mathcal{T}[p^*, q^*]$ as the optimal subtrajectory.

Our algorithm to compute $\mathcal{T}[p^*, q^*]$ consists of five steps. In Section 5.1, we construct a discrete set S of candidate starting points on \mathcal{T} . In Section 5.2, we prove $p^* \in S$, where p^* is the starting point of the optimal trajectory and S is the set of candidate starting points. In Section 5.3, we generalise the notion of the reach, and we generalise Lemma 13 to obtain an algorithm for computing the reach. In Section 5.4 we show how to compute all six types of candidate starting points efficiently. Finally, in Section 5.6, we compute the reach of all candidate starting points to obtain the optimal subtrajectory.

5.1 Identifying the set of starting points

In this section we identify a discrete set S of candidate starting points on \mathcal{T} . In the subsequent section we prove $p^* \in S$. We define six types of events, depending on different types of starting points, as follows. Given a trajectory \mathcal{T} , p is a

vertex event (see Figure 18 (left)) if and only if

p is a vertex of \mathcal{T} .

reach event (see Figure 18 (middle)) if and only if

$r(p)$ is a vertex of \mathcal{T} , and no point $q \prec p$ satisfies $r(q) = r(p)$.

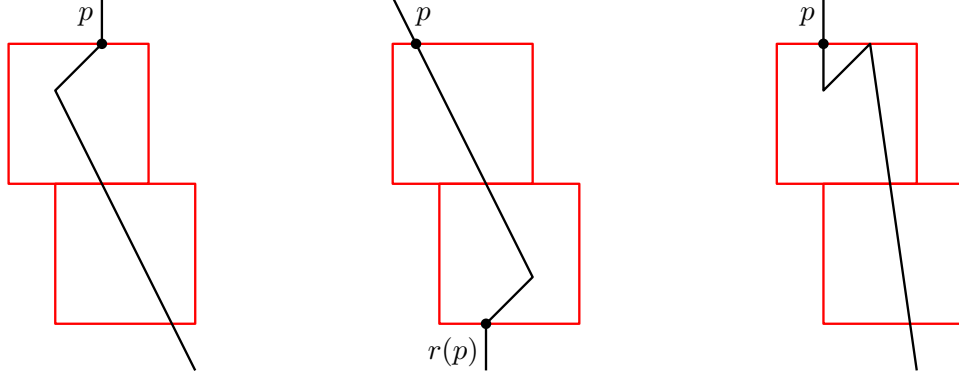


Figure 18: A vertex event (left), a reach event (middle), and a bounding box event (right).

bounding box event (see Figure 18 (right)) if and only if the topmost vertex of \mathcal{T} within the subtrajectory $\mathcal{T}[p, r(p)]$ has the same y -coordinate as p .

bridge event (see Figure 19 (left)) if and only if

- the point p is the leftmost point on $\mathcal{T}[p, r(p)]$, and
- the point p is one unit to the left of a point $u \in \mathcal{T}[p, r(p)]$, and
- the point u is one unit above the lowest vertex of \mathcal{T} in the subtrajectory $\mathcal{T}[p, r(p)]$.

upper envelope event (see Figure 19) if and only if

- the point p is the leftmost point on $\mathcal{T}[p, r(p)]$, and
- the point p is one unit to the left of a point $u \in \mathcal{T}[p, r(p)]$, and
- the point u is an vertex on the upper envelope of $\mathcal{T}[p, r(p)]$.

special configuration event (see Figure 20) if and only if

there is a covering of squares \mathcal{H}_1 and \mathcal{H}_2 so that \mathcal{H}_1 contains the top-left corner of \mathcal{H}_2 , and either:

- point p is in the top-right corner of \mathcal{H}_1 and $r(p)$ is in the bottom-left corner of \mathcal{H}_1 , or
- point p is in the top-left corner of \mathcal{H}_1 and the trajectory \mathcal{T} passes through the bottom-right corner of \mathcal{H}_1 , or
- point p is in the top-left corner of \mathcal{H}_1 , $r(p)$ is in the bottom-right corner of \mathcal{H}_2 , and the trajectory \mathcal{T} passes through the two intersections of \mathcal{H}_1 and \mathcal{H}_2 .

Next, we use these six event types to define the set of candidate starting points in Definition 1. Note that in Definition 1, we generalise bounding box, bridge, upper envelope and special configuration events to include the events for all four cardinal directions, not just the upwards cardinal direction. For example, a point p for which the bottom-most vertex of $\mathcal{T}[p, r(p)]$ also has y -coordinate p_y is also a bounding box event.

Definition 1. Let \mathcal{T}_1 be a copy of \mathcal{T} with the following additional points added to the set of vertices of \mathcal{T}_1 :

- all the vertex, reach, bounding box, and bridge events of \mathcal{T} for all four cardinal directions.

Next, let \mathcal{T}_2 be a copy of \mathcal{T}_1 with the following additional points added to the set of vertices of \mathcal{T}_2 :

- all the upper envelope events of \mathcal{T}_1 for all four cardinal directions.

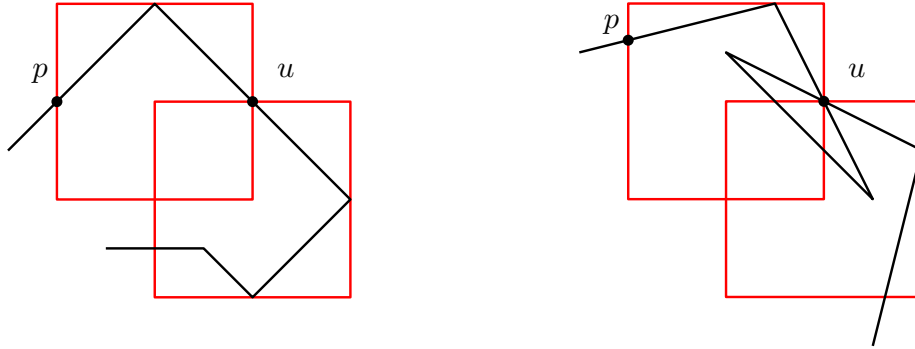


Figure 19: Examples of a bridge event (left), and an upper envelope event box (right).

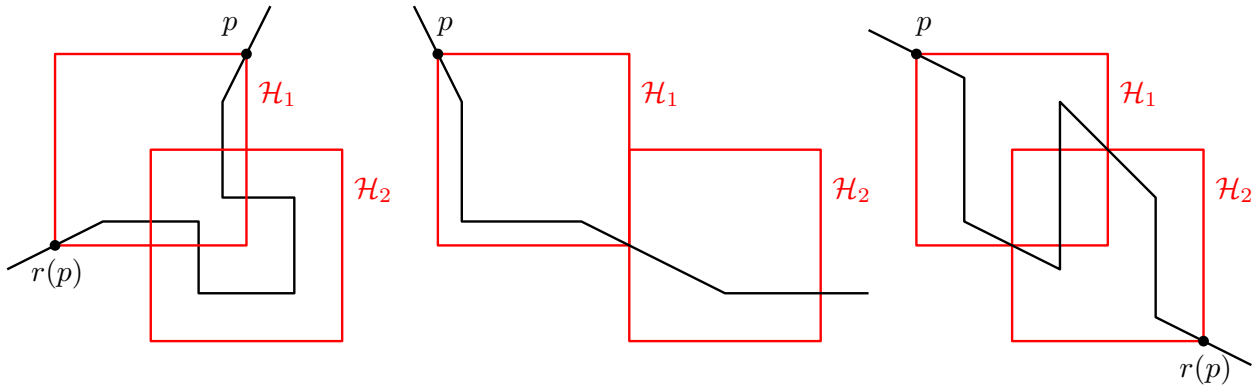


Figure 20: Examples of the three types of special configuration events.

Finally, let \mathcal{T}_3 be a copy of \mathcal{T}_2 with the following additional points added to the set of vertices of \mathcal{T}_3 :

- all the special configuration events of \mathcal{T}_2 for all configurations of \mathcal{H}_1 and \mathcal{H}_2 .

Finally, we define S to be the vertices of \mathcal{T}_3 . This completes the characterization of S , the set of candidate starting points.

5.2 Proof that $p^* \in S$

In this section, we prove that the starting point p^* of the optimal subtrajectory is a candidate starting point in S . Our main strategy is to argue that if p^* is not a vertex of \mathcal{T}_2 , either p^* or q^* must be in a corner of one of the two squares (Lemma 16). Using a careful analysis, we then argue that the solution must actually be a special configuration event, and thus $p^* \in S$. Next, we define bridging points, which help us to establish some useful technical lemmas.

Given a point p , a point $t \in \mathcal{T}[p, r(p)]$ is said to be a *bridging point* for point p if there exists covering $\mathcal{H}_1 \cup \mathcal{H}_2$ of $\mathcal{T}[p, r(p)]$ so that, assuming p is on the boundary of \mathcal{H}_1 :

- The point t lies on the boundary of both \mathcal{H}_1 and \mathcal{H}_2 , and
- The points t and p are on opposite sides of \mathcal{H}_1 .

See Figure 21 for an example. For a covering $\mathcal{H}_1 \cup \mathcal{H}_2$ of $\mathcal{T}[p, r(p)] = \mathcal{T}[p, q]$, a side of \mathcal{H}_1 and \mathcal{H}_2 that contains p (respectively q) is a p -*side* (respectively q -*side*). A side that contains a bridging

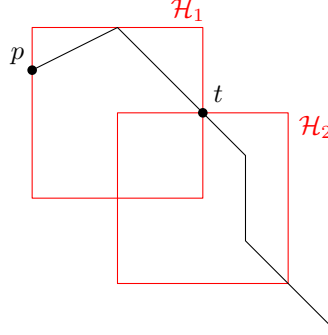


Figure 21: An example of a bridging point t for the starting point p .

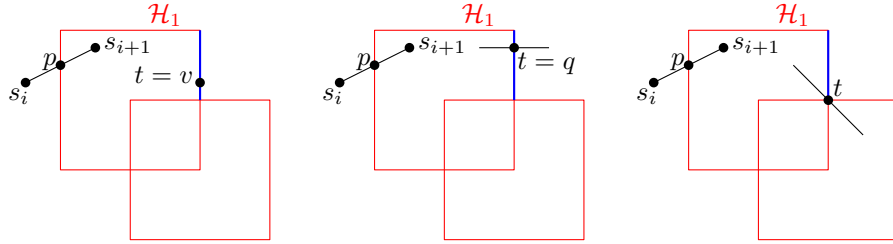


Figure 22: The three cases for the point t that is lost when moving \mathcal{H}_1 to the left.

point is a b -side. If two sides are part of the same square and have the same orientation (vertical or horizontal), they are opposite to each other.

Observation 2. A bridging point x either lies on both the upper and right envelopes of the subtrajectory, or on both the lower and left envelopes of the subtrajectory.

Lemma 14. Let $\mathcal{T}[p, q]$ be an optimal 2-coverable subtrajectory and assume that p is not a vertex of \mathcal{T}_2 . There is a covering of $\mathcal{T}[p, q]$ by squares $\mathcal{H}_1 \cup \mathcal{H}_2$ so that any side opposite to a p -side must either be a b -side or a q -side.

Proof. Assume without loss of generality that p lies on the left side of \mathcal{H}_1 . We now argue that the right side of \mathcal{H}_1 is a b -side or a q -side.

Since p is not a vertex of \mathcal{T}_2 , it lies between two consecutive vertices s_i and s_{i+1} of \mathcal{T}_2 , as shown in Figure 22. The segment $s_i s_{i+1}$ is a line segment. Consider the situation if we moved \mathcal{H}_1 to the left by an arbitrarily small amount. This would allow us to cover additional length of $s_i s_{i+1}$ on the left side of \mathcal{H}_1 . Since $\mathcal{T}[p, q]$ is optimal, there must be a point $t \in \mathcal{T}[p, q]$ on the right side of \mathcal{H}_1 that does not lie in the interior of \mathcal{H}_2 which is lost even as we move left by an arbitrarily small amount. There are three possible cases for this point t , as shown in Figure 22:

Case t is a vertex v of \mathcal{T} : This would make p an upper envelope event for vertex v . This would mean that p is a vertex of \mathcal{T}_2 , which contradicts the lemma statement. Hence, this case cannot actually occur.

Case t is point q : This means the right side of \mathcal{H}_1 is a q -side, as desired.

Case t is an interior point of \mathcal{T} : This means \mathcal{T} , in particular $\mathcal{T}[p, q]$, continues into \mathcal{H}_2 at t . This means t must lie on the boundary of \mathcal{H}_2 , and thus the right side of \mathcal{H}_1 is a b -side, as desired.

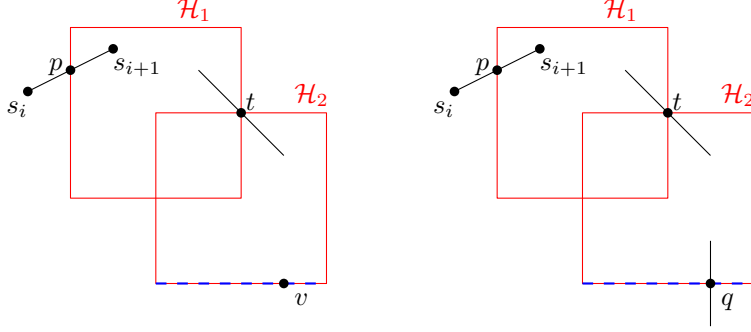


Figure 23: Cases when the point p is not in a corner and there is a bridging point.

Note that if p lies on a corner of \mathcal{H}_1 , say e.g. the top-left corner, there are two p -sides. Using the same argument as above, it then follows that the bottom-side of \mathcal{H}_1 must also either be a q -side or a b -side. \square

Lemma 15. *Let $\mathcal{T}[p, q]$ be an optimal 2-coverable subtrajectory and assume that p is not a vertex of \mathcal{T}_2 . There is a covering of $\mathcal{T}[p, q]$ by squares $\mathcal{H}_1 \cup \mathcal{H}_2$ so that any side of \mathcal{H}_2 opposite to a b -side must be a q -side.*

Proof. Let t be a bridging point that lies on the right side of \mathcal{H}_1 , and the top side of \mathcal{H}_2 . The other cases are symmetric. We then have to show that the bottom side of \mathcal{H}_2 is a q -side.

To this end we move \mathcal{H}_1 left by an arbitrarily small amount and then move \mathcal{H}_2 upwards by an arbitrarily small amount to cover the neighborhood of the bridging point. By the same argument as in Lemma 14, there must be a point on $\mathcal{T}[p, q]$ that we lost on the bottom edge of \mathcal{H}_2 . There are two cases as shown in Figure 23.

The first case is if the point on the bottom edge of \mathcal{H}_2 is a vertex. Refer to the left diagram in Figure 23. This would make p a bridge event and thus a vertex of \mathcal{T}_2 , which would be a contradiction. Thus, the trajectory \mathcal{T} must exit the covering $\mathcal{H}_1 \cup \mathcal{H}_2$ on the bottom edge. The point on the bottom edge is q and so the bottom side of \mathcal{H}_2 is a q -side, as required.

In case t also lies on a second side of \mathcal{H}_2 , say the left side, then we also have to argue that the right side of \mathcal{H}_2 is a q -side. Suppose that the right side of \mathcal{H}_2 does not contain q , then it must contain a vertex w of $\mathcal{T}[p, r(p)]$ (otherwise we could again shift \mathcal{H}_2 left). However, since p lies on the left side of \mathcal{H}_1 (by definition of t), this would make p a reach event of w , and thus a vertex of \mathcal{T}_2 . Contradiction. \square

Next we use the above lemmas to show that either p or q is in a corner of \mathcal{H}_1 or \mathcal{H}_2 .

Lemma 16 (The corner lemma). *Suppose p is not a vertex of \mathcal{T}_2 and $\mathcal{T}[p, q]$ is optimal. Then we have that either p is in a corner of \mathcal{H}_1 or \mathcal{H}_2 or that q is in a corner of \mathcal{H}_1 or \mathcal{H}_2 .*

Proof. We assume by contradiction that that p is not a vertex of \mathcal{T}_2 , and there is a covering $\mathcal{H}_1 \cup \mathcal{H}_2$ of the subtrajectory $\mathcal{T}[p, q]$ where neither of p nor q are in a corner of \mathcal{H}_1 or \mathcal{H}_2 . We show that this implies that the subtrajectory $\mathcal{T}[p, q]$ cannot be optimal.

We have two cases. Either the point p lies on the left side of \mathcal{H}_1 or the right side of \mathcal{H}_1 . All other cases are symmetric.

Case 1: p is on the left side of \mathcal{H}_1 . The left side of \mathcal{H}_1 is a p -side, so by Lemma 14, the right side of \mathcal{H}_1 is either a q -side or a b -side. We consider two subcases.

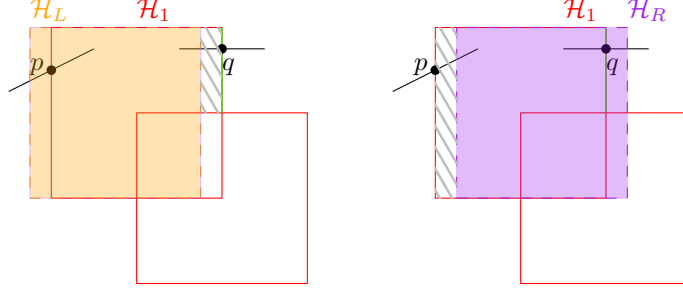


Figure 24: The new squares \mathcal{H}_L and \mathcal{H}_R are constructed to the left and right of \mathcal{H}_1 respectively.

Case 1.1: p is on the left side of \mathcal{H}_1 and q is on the right side. See Figure 24.

We show that $\mathcal{T}[p, q]$ cannot be optimal by constructing an earlier subtrajectory with the same length as $\mathcal{T}[p, q]$. We do this by constructing a subtrajectory covered by a square slightly to the left of \mathcal{H}_1 , and another subtrajectory covered by a square slightly to the right of \mathcal{H}_1 .

If there is a vertex on the left side of \mathcal{H}_1 , then

that would make p a bounding box event and a vertex of \mathcal{T}_1 . If there is a vertex on the right side of \mathcal{H}_1 , then

that would make p an upper envelope event and vertex of \mathcal{T}_2 . Since p is not a vertex of \mathcal{T}_2 , we must have that there are no vertices on the left side or the right side of \mathcal{H}_1 .

Now, take \mathcal{H}_1 and move it left and right by the same arbitrarily small amount, and call these new squares \mathcal{H}_L and \mathcal{H}_R respectively. For \mathcal{H}_L on the left diagram of Figure 24, because there are no vertices or bridging points on the right edge, we can choose the movement small enough so that the gray diagonally shaded region is empty. We can do the same for \mathcal{H}_R on the right diagram, because there are no vertices on the left edge, so we can choose the movement small enough so that the gray diagonally shaded region is also empty. So the only lengths gained or lost are those on the segment e_p that contains p , or the segment e_q that contains q .

Suppose that $\mathcal{T}[p, q]$ has length L and by assumption is maximal. Let the length of trajectory we gain with \mathcal{H}_L on segment e_p be ℓ_p and the length of trajectory we lose on segment e_q be ℓ_q . By symmetry and the fact that p and q are not in corners of \mathcal{H}_1 , we have that \mathcal{H}_R loses the same amount ℓ_p and gains the same amount ℓ_q . Therefore, we have trajectories close to $\mathcal{T}[p, q]$ with lengths L , $L - \ell_p + \ell_q$ and $L + \ell_p - \ell_q$ respectively. Since L is maximal, we must have $\ell_p = \ell_q$. But now we have an earlier trajectory with the same length as $\mathcal{T}[p, q]$, so $\mathcal{T}[p, q]$ is not optimal.

Case 1.2: p is on the left side of \mathcal{H}_1 and there is a bridging point on the right side. See Figure 25.

It follows from Observation 2 that this bridging point must lie on the top side of \mathcal{H}_2 (as it must lie on the upper and right envelopes of $\mathcal{T}[p, r(p)]$). Then, Lemma 15 tells us that the bottom side of \mathcal{H}_2 must be a q -side.

We now follow a similar shifting argument as before. This time we shift both \mathcal{H}_1 and \mathcal{H}_2 . We move \mathcal{H}_1 left to form \mathcal{H}_{L_1} , and \mathcal{H}_2 up to form \mathcal{H}_{L_2} and cover the part of the upper envelope left uncovered by \mathcal{H}_{L_1} . We apply the opposite movements to obtain \mathcal{H}_{R_1} and \mathcal{H}_{R_2} respectively.

Again, the gray regions on the left and right sides of \mathcal{H}_1 are empty if we choose the movement small enough, otherwise p would be a vertex of \mathcal{T}_2 . For \mathcal{H}_2 we have an analogous reason but

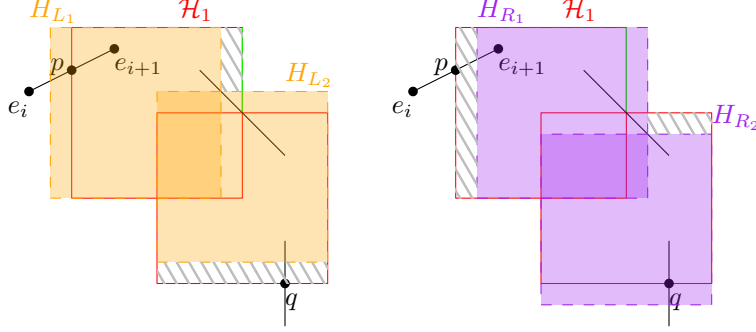


Figure 25: New hotspot positions for starting slightly before and after p .

this time it would make q a vertex of \mathcal{T}_2 . Therefore, the only parts of the trajectory gained or lost are those close to p or q . By the same argument as before, these lengths ℓ_p and ℓ_q are the same for $\mathcal{H}_{L1} \cup \mathcal{H}_{L2}$ and $\mathcal{H}_{R1} \cup \mathcal{H}_{R2}$. Therefore, we again deduce that in order for $\mathcal{T}[p, q]$ to be optimal, ℓ_p and ℓ_q must be equal, but then $\mathcal{T}[p, q]$ is not the earliest optimal trajectory.

Case 2: p is on the right side of \mathcal{H}_1 . By Lemma 14, the left side of \mathcal{H}_1 is a q -side, since it cannot be a b -side (by Observation 2). The proof of this case is exactly the same as Case 1. We use the same construction as the one shown in Figure 24.

In all cases, if p is not a vertex of \mathcal{T}_2 and p and q are not in corner positions of \mathcal{H}_1 and \mathcal{H}_2 , then $\mathcal{T}[p, q]$ is not an optimal subtrajectory. \square

Finally, we show that p is not only a corner of \mathcal{H}_1 or \mathcal{H}_2 , but also that p is in fact a special configuration event.

Lemma 17. *Suppose that $\mathcal{T}[p, q]$ is optimal and that p is not a vertex of \mathcal{T}_2 . Then p is a special configuration event.*

Proof. By Lemma 16, we must have p or q be in a corner of \mathcal{H}_1 or \mathcal{H}_2 . Without loss of generality, suppose that p is in a corner of \mathcal{H}_1 . Up to rotation this leaves only two cases, either p is in the top-left corner of \mathcal{H}_1 , or p is in the top-right corner of \mathcal{H}_1 .

Case 1: p is in the top-left corner. Consider the sides opposite to p on \mathcal{H}_1 . These would be the bottom side and right side of \mathcal{H}_1 . Lemma 14 implies both these sides must contain either q or a bridging point. Since $\mathcal{T}[p, r(p)]$ enters \mathcal{H}_2 , at least one of these two sides must contain a bridging point.

Moreover, applying Lemma 15 to the bridging point implies that q is in fact on the square \mathcal{H}_2 and not \mathcal{H}_1 . Therefore, both sides opposite p contain a bridging point, and q is on \mathcal{H}_2 . There are two subcases. Either there are two different bridging points on the bottom and right sides of \mathcal{H}_1 , or there is a single bridging point in the bottom-right corner of \mathcal{H}_1 . See Figure 26.

In the first subcase, there are two different bridging points on the bottom and right sides of \mathcal{H}_1 , see Figure 26 left. Therefore, there are two bridging points, on the top and left edges of \mathcal{H}_2 . We apply Lemma 15 on the two bridging points. The bridging point on the top edge of \mathcal{H}_2 implies that q must be on the bottom edge of \mathcal{H}_2 , whereas the bridging point on the left edge implies that q must be on the right edge of \mathcal{H}_2 . So q is in the bottom-right corner of \mathcal{H}_2 . Therefore, p is a special configuration event.

In the second subcase, there is a single bridging point in the bottom-right corner of \mathcal{H}_1 . See Figure 27 right. This makes p a special configuration event.

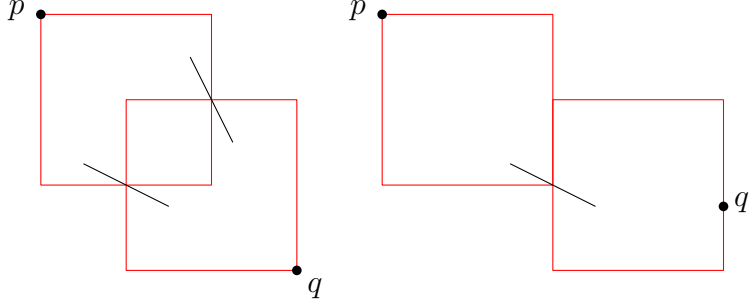


Figure 26: The special configuration events in Case 1.

Case 2: p is in the top-right corner. Lemma 14 implies that the left and bottom edges of \mathcal{H}_1 must contain either q or a bridging point. However, by Observation 2, the left edge of \mathcal{H}_1 cannot contain a bridging point, and thus q lies on \mathcal{H}_1 . Supposing there was a bridging point on the bottom edge of \mathcal{H}_1 , Lemma 15 would again imply that q is on the right edge of \mathcal{H}_2 , contradicting the fact that q is on the left edge of \mathcal{H}_1 . Therefore, there are no bridging points, p is in the top-right corner of \mathcal{H}_1 and q is on the bottom-left corner of \mathcal{H}_1 . See Figure 27. This makes p a special configuration event.

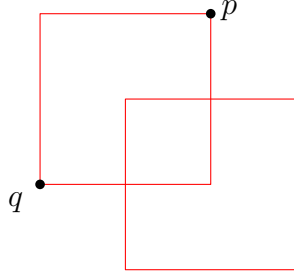


Figure 27: The special configuration event in Case 2.

□

By Lemma 17, the starting point of the optimal subtrajectory is either a vertex of \mathcal{T}_2 or a special configuration event. Hence, the starting point p^* of the optimal subtrajectory must be a vertex of \mathcal{T}_3 , and thus $p^* \in S$. We summarise with the following Theorem.

Theorem 7. *The set S of vertices of \mathcal{T}_3 is guaranteed to contain the starting point of a longest coverable subtrajectory of \mathcal{T} .*

5.3 Computing the reach of a point

In this section we describe how, given a candidate starting point p , we can compute the longest 2-coverable subtrajectory starting at p . We modify the data structure in Theorem 4, i.e. the data structure for answering whether a given subtrajectory is 2-coverable, to answer such reach queries. We do so by applying parametric search to the query procedure. Note that applying a simple binary search will give us only the edge containing $r(p)$. Furthermore, even given this edge it is unclear how to find $r(p)$ itself, as the squares may still shift, depending on the exact position of $r(p)$.

Lemma 18. *Let \mathcal{T} be a trajectory with n vertices. After $O(n\alpha(n)\log n)$ preprocessing time, \mathcal{T} can be stored using $O(n\alpha(n)\log n)$ space, so that given a query point p on \mathcal{T} it can compute the reach $r(p)$ of p in $O(\log^2 n)$ time.*

Proof. We would like to compute the maximum value $q \in [0, 1]$ so that $\mathcal{T}[p, q]$ is 2-coverable. The decision version of this optimisation problem is to decide whether a given subtrajectory $\mathcal{T}[p, q]$ is 2-coverable. This decision version is monotone since for any q' with $q < q'$, the subtrajectory $\mathcal{T}[p, q']$ contains the subtrajectory $\mathcal{T}[p, q]$. After $O(n\alpha(n)\log n)$ preprocessing time Theorem 4 gives us a comparison-based algorithm, the query procedure, that solves the decision problem in $O(\log n)$ time. The sequential version of parametric search [14] states that if T is the running time of the sequential algorithm, the optimisation algorithm takes $O(T^2)$ time. In our case, the reach can be answered in $O(\log^2 n)$ time as required. \square

Corollary 1. *Given a trajectory \mathcal{T} , and a set of m candidate starting points on \mathcal{T} , we can compute the longest 2-coverable subtrajectory that starts at one of those points in $O(n\alpha(n)\log n + m\log^2 n)$ time.*

5.4 Computing the set of starting points

Next, we bound the number of events, and thus the number of candidate starting points. We also provide algorithms for computing the events, and we analyze the running times of our algorithms. Combining this with our result from Corollary 1 gives us an efficient algorithm to compute the optimal 2-coverable subtrajectory. Section 5.4.1 is dedicated to reach events, Section 5.4.2 to bounding box events, Section 5.4.3 to bridge events, Section 5.4.4 to upper envelope events, and Section 5.4.5 to special configuration events.

5.4.1 Reach events

Lemma 19. *Given a trajectory with n vertices, there are at most $O(n)$ reach events which can be computed in $O(n\log^2 n)$ time.*

Proof. Suppose p is a reach event and $r(p)$ is a vertex. The vertex $r(p)$ uniquely defines p since it is the earliest point on the trajectory \mathcal{T} that reaches $r(p)$. Since there are n vertices, there are at most $O(n)$ reach events.

The running time is immediately implied by Corollary 1, as we are computing the reaches of all the vertices. \square

5.4.2 Bounding box events

Lemma 20. *Given a trajectory with n vertices, there are at most $O(n)$ bounding box events.*

Proof. Suppose p is such a bounding box event. Let the first and last vertices of \mathcal{T} in the subtrajectory $\mathcal{T}[p, r(p)]$ be v_i and v_j . We prove that the pair of vertices v_i and v_j uniquely determines p . Then we prove that there are at most $O(n)$ possible choices of the pair v_i and v_j .

Suppose v_i and v_j are given. Let v_{i-1} be the vertex preceding v_i , then p must lie on the segment $v_{i-1}v_i$. The vertex v_L is the unique leftmost vertex between v_i and v_j . Now, v_L determines the x -coordinate of p , and since p lies on $v_{i-1}v_i$, we have the unique position for p . Therefore, the vertices v_i and v_j uniquely determine p .

Analogous to in Section 4 there are $O(n)$ relevant pairs of vertices v_i, v_j that we have to consider, and each pair (v_i, v_j) uniquely determines the bounding box event p , we have that there are at most $O(n)$ bounding box events. \square

Lemma 21. *Given a trajectory with n vertices, one can compute all bounding box events in $O(n \log^2 n)$ time.*

Proof. From the proof in Lemma 20, we know that p can be determined by the pair (v_i, v_j) . We also proved the relationship between the pair (v_i, v_j) and the longest coverable vertex-to-vertex subtrajectory starting at either v_i or ending at v_j . As a consequence of Lemma 18, we can compute all longest coverable vertex-to-vertex subtrajectories starting at each vertex v_i in $O(n \log^2 n)$ time. Those ending at vertex v_j can be handled analogously.

For each of the $O(n)$ pairs of vertices (v_i, v_j) we use the same method as in Lemma 20 to determine the bounding box event p . We use the bounding box data structure to query v_L in $O(\log n)$ time. This determines the x -coordinate of p . Then we compute p by computing the intersection of the two lines: the vertical line through v_L and the trajectory edge $v_{i-1}v_i$. \square

5.4.3 Bridge events

Lemma 22. *Given a trajectory with n vertices, there are at most $O(n)$ bridge events.*

Proof. Let the first and last vertices in the subtrajectory $\mathcal{T}[p, r(p)]$ be v_i and v_j . By Lemma 20, there are $O(n)$ relevant pairs of vertices (v_i, v_j) . It suffices to show that for each pair (v_i, v_j) there are only a constant number of bridge events. The pair (v_i, v_j) determines the leftmost vertex v_L on $\mathcal{T}[v_i, v_j]$. If x is in $\mathcal{T}[v_i, v_j]$ then it is the unique point on the upper envelope of $\mathcal{T}[v_i, v_j]$ one unit to the right of v_L . Otherwise, x is on $v_{i-1}v_i$ or v_jv_{j+1} and one unit to the right of v_L . There are at most two possible positions for the bridging point x . Thus there are a constant number of bridge events for each of the $O(n)$ pairs (v_i, v_j) . \square

Lemma 23. *Given a trajectory with n vertices, one can compute all bridge events in $O(n \log^2 n)$ time.*

Proof. In a similar manner to the proof of Lemma 21, we begin by computing all pairs (v_i, v_j) in $O(n \log^2 n)$ time. For each pair (v_i, v_j) we compute the vertex v_L in $O(\log n)$ time with the bounding box data structure. Consider two cases. If x is in $\mathcal{T}[v_i, v_j]$ we query the upper envelope of $\mathcal{T}[v_i, v_j]$ in $O(\log n)$ time with the upper envelope data structure. Otherwise, if x is not in $\mathcal{T}[v_i, v_j]$, then x is on $v_{i-1}v_i$ or v_jv_{j+1} and we can compute the intersection in $O(1)$ time using $\mathcal{BB}(\mathcal{T}[v_i, v_j])$. Therefore, the running time is $O(n \log^2 n)$ time in total. \square

5.4.4 Upper envelope events

Lemma 24. *Given a trajectory with n vertices, there are $O(n2^{\alpha(n)})$ upper envelope events of \mathcal{T} , where α is the inverse Ackermann function.*

Proof. For each upper envelope event p of the trajectory \mathcal{T} , let $u(p)$ be the segment of \mathcal{T} on the upper envelope of $\mathcal{T}[p, r(p)]$ that is one unit to the right of p . If there are multiple such segments, take any of them. As p ranges from the earliest upper envelope event to the last one, $u(p)$ is a sequence of segments. It suffices to show that $u(p)$ is bounded from above by $O(n2^{\alpha(n)})$. We achieve this by showing that the sequence of segments $u(p)$ is a Davenport-Schinzel sequence of order $s = 4$ [19].

Recall that a Davenport-Schinzel sequence of order $s = 4$ has no alternating subsequences of length $s + 2 = 6$. The subsequence cannot occur anywhere in the sequence even for non-consecutive appearance of the terms. Our first step is to show that if the sequence a, b, a occurs (not necessarily consecutively) then the first two elements of the sequence must be x -monotone, in that the first

element is to the left of the second element. Our second step is to deduce a contradiction from an alternating and x -monotone subsequence of length five.

Suppose that a, b, a is a subsequence of $u(p)$, then there exists three upper envelope events $p_1 \prec p_2 \prec p_3$ along the trajectory \mathcal{T} so that $u(p_1), u(p_2), u(p_3) = a, b, a$. In other words, segment $a = u(p_1) = u(p_3)$ whereas segment $b = u(p_2)$. Suppose for the sake of contradiction that p_2 is to the left of p_1 . See Figure 28.

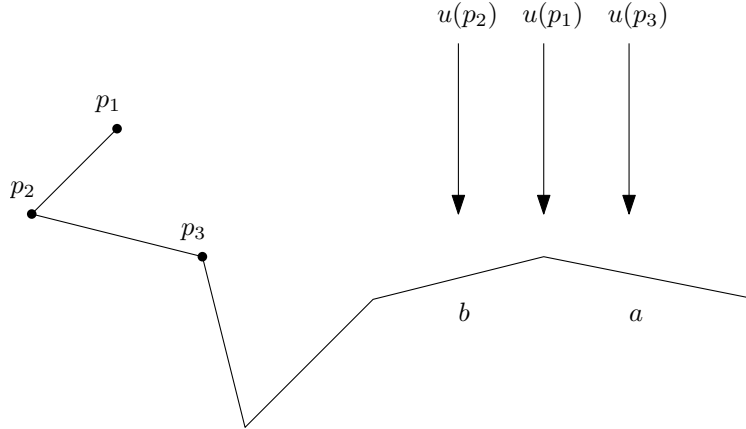


Figure 28: Three upper envelope events p_1, p_2, p_3 so that $u(p_1), u(p_2), u(p_3)$ are alternating.

Recall that since p_1 is an upper envelope event, p_1 is the leftmost point of $\mathcal{T}[p_1, r(p_1)]$. But p_2 is to the left of p_1 , so we must have that $p_2 \notin \mathcal{T}[p_1, r(p_1)]$, and therefore $r(p_1) \prec p_2$. Moreover, for any point p , we have $p \prec u(p) \prec r(p)$. Combining these, we get:

$$u(p_1) \prec r(p_1) \prec p_2 \prec p_3 \prec u(p_3) = u(p_1).$$

This is a contradiction, so p_1 is to the left of p_2 . Therefore, whenever the alternating subsequence $u(p_1), u(p_2), u(p_3) = a, b, a$ occurs, the first two elements p_1 and p_2 are x -monotone.

Now suppose we have an alternating subsequence a, b, a, b, a, b of length 6. Let the subsequence be $u(p_1), u(p_2), u(p_3), g(p_4), g(p_5), g(p_6)$. By the property above, we have that p_1, p_2, p_3, p_4 and p_5 are x -monotone. Since $u(p_1) = g(p_5) = a$, the segment a spans the entire x -interval from $u(p_1)$ to $g(p_5)$. But now $u(p_2) = g(p_4) = b$, which means that segment b is above segment a at $u(p_2)$ and $g(p_4)$. Since a and b are straight, this implies that b is also above a at $u(p_3)$. But $u(p_3) = a$, which is a contradiction. Therefore the alternating subsequence of length 6 does not occur and $u(p)$ is a Davenport-Schinzel sequence of order $s = 4$. \square

Lemma 25. *Given a trajectory with n vertices, one can compute all upper envelope events in $O(n\alpha(n)\log^2 n)$ time.*

Proof. We begin with a preprocessing step. We compute a set S of all vertex events, reach events, and bounding box events of \mathcal{T} . Since there is one reach event per vertex there are $O(n)$ reach events, and combined with Lemma 24, this means that S has size $O(n)$.

The set S has three properties. The first property is that between any two consecutive events s_i and s_{i+1} , the trajectory \mathcal{T} is a straight segment, since all vertices of \mathcal{T} are in S . The second property is that for the set of points $p \in \mathcal{T}[s_i, s_{i+1}]$, their set of reaches $\{r(p) : p \in \mathcal{T}[s_i, s_{i+1}]\}$ must lie on a straight segment of \mathcal{T} . The reason for this is that if there were a vertex strictly between $r(s_i)$ and $r(s_{i+1})$, then there would be a (reach) event between s_i and s_{i+1} , contradicting the fact that s_i and s_{i+1} are consecutive. Finally, the third property is that, supposing s_i is the leftmost

point on the subtrajectory $\mathcal{T}[s_i, r(s_i)]$, then for any $p \in \mathcal{T}[s_i, s_{i+1}]$, p is the leftmost point on the subtrajectory $\mathcal{T}[p, r(p)]$. The reason for this is that if there were p that had a vertex v to the left of p , then there would be a bounding box event strictly between s_i and s_{i+1} .

Next, we extend these properties of S to properties of upper envelope events that are between s_i and s_{i+1} . Let v_i and v_j be the first and last vertices of $\mathcal{T}[p, r(p)]$ for some point $p \in \mathcal{T}[s_i, s_{i+1}]$. As a consequence of the first two properties of set S , the vertices v_i and v_j are the same regardless of our choice of point p . Now suppose that p is an upper envelope event. This means that p is to the left of all vertices on the subtrajectory $\mathcal{T}[v_i, v_j]$. As a consequence of the third property of set S , both s_i and s_{i+1} have x -coordinate less than or equal to the x -coordinate of all vertices of the subtrajectory $\mathcal{T}[v_i, v_j]$.

Now the algorithm is to take each pair of consecutive events (s_i, s_{i+1}) and compute the upper envelope events that occur between s_i and s_{i+1} . We decide on a subset of these pairs (s_i, s_{i+1}) to skip, since they will have no upper envelope events. For each pair of consecutive events (s_i, s_{i+1}) , compute the vertices v_i and v_j (which are the first and last vertices of $\mathcal{T}[p, r(p)]$ for any point $p \in \mathcal{T}[s_i, s_{i+1}]$). From the definition of an upper envelope event we have that the first requirement on an upper envelope p implies that p is to the left of the entire subtrajectory $\mathcal{T}[v_i, v_j]$. This implies that if the segment $s_i s_{i+1}$ is not entirely to the left of $\mathcal{T}[v_i, v_j]$, we can skip the pair (s_i, s_{i+1}) .

The second requirement is that p is one unit to the right of an inflection point u on the upper envelope of $\mathcal{T}[v_i, v_j]$. In particular, if x_i and x_{i+1} are the x -coordinates of s_i and s_{i+1} , then computing the upper envelope events p in the vertical strip $[x_i, x_{i+1}]$ is equivalent to computing the inflection points u in the vertical strip $V = [x_i + 1, x_{i+1} + 1]$.

Our problem is now to compute the upper envelope of $\mathcal{T}[v_i, v_j]$ in the vertical strip V . For each of the $O(\log n)$ canonical subsets of the subtrajectory $\mathcal{T}[v_p, v_q]$, we compute the upper envelope Γ_i for that canonical subset. The upper envelope of $\mathcal{T}[v_i, v_j]$ is simply the upper envelope of the $O(\log n)$ upper envelopes Γ_i . In order to argue amortised complexity for computing the upper envelope of the Γ_i 's, we proceed with a sweepline algorithm.

Suppose our vertical sweepline is ℓ . Let its initial state ℓ_{start} be the left boundary of V , and its ending state ℓ_{end} be the right boundary of V . We maintain three invariants for the sweepline ℓ . First, we maintain pointers p_i to mark the positions and directions of each of the Γ_i . Second, we maintain the current highest of the pointers p_i , which we will call p_{max} . Finally, we maintain possible intersections where p_{max} may change, as such we maintain the intersection of p_{max} with each other p_i . See Figure 29.

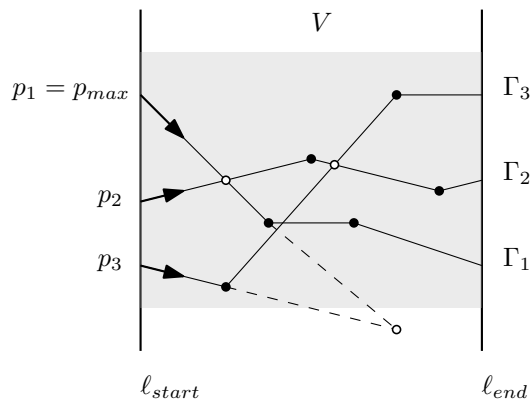


Figure 29: Sweepline maintains pointers p_i . Solid dots: p_i changes. Hollow dots: p_{max} swaps.

There are two types of sweepline events. The first type of sweepline event occurs when a

pointer p_i changes. These sweepline events are marked with solid dots in Figure 29, and are the inflection points of Γ_i . In our update step, we update the pointer p_i and the intersection(s) between p_{max} and p_i . The second type of sweepline event occurs p_{max} changes, in particular when it swaps with some other pointer p_i . These intersection points are marked with hollow dots in Figure 29. In our update step, we update p_{max} and all intersections between p_{max} and p_i .

Once the sweepline algorithm terminates, the segments traced by the pointer p_{max} corresponds to the upper envelope of $\mathcal{T}[v_i, v_j]$. We compute the inflection points along p_{max} and our algorithm returns all upper envelope events p on $s_i s_{i+1}$ which are one unit to the left of an inflection point.

It remains to analyse the amortised running time of this algorithm. By Corollary 1 we can compute a reach event for each vertex in $O(n \log^2 n)$ time. By Lemma 21 we can compute all bounding box events in $O(n \log^2 n)$. We construct the upper envelope of all canonical subsets of \mathcal{T} in $O(n \log^2 n)$ time [10]. We initialise the sweepline algorithm and compute all $O(\log n)$ pointers in $O(\log^2 n)$ time. When the direction of a pointer changes, we update the pointer in constant time, and calculate the new intersections between p_{max} and p_i . Since each new intersection can be computed in constant time, and there are $O(\log n)$ intersections to calculate, this step takes $O(\log n)$ time. When the highest pointer p_{max} changes, we update p_{max} in constant time, and calculate new intersections in $O(\log n)$ time. Therefore, the amortised running time of the sweepline algorithm is $O(\log n)$ per sweepline event. Hence, it suffices to count the number of sweepline events.

The first type of sweepline event is when the direction of the pointer p_i changes. The number of times a pointer p_i changes is equal to the number of inflection points of Γ_i in the vertical strip V . Suppose that we charge the sweepline event to that inflection point on Γ_i . If we show that each inflection point on Γ_i gets charged at most once, not just during a single sweepline algorithm but in total across all pairs (s_i, s_{i+1}) , then the total number of sweepline events of this type is bounded by the total complexity of all the Γ_i 's. The total complexity of all upper envelopes of all canonical subsets of the trajectory is $O(n\alpha(n) \log n)$ [10].

Suppose for a sake of contradiction that two sweepline events charge to the same inflection point u . Since the sweepline algorithm sweeps from left to right without backtracking, these two sweepline events must have originated from two different pairs.

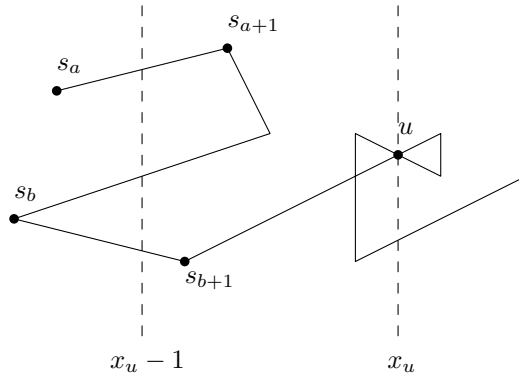


Figure 30: If s_b is after s_{a+1} , then s_b contradicts the leftmost point property of s_{a+1} .

Suppose that the inflection point u is charged by sweepline events originating from pairs (s_a, s_{a+1}) and (s_b, s_{b+1}) . Without loss of generality let $s_a \prec s_{a+1} \prec s_b$ along the trajectory \mathcal{T} . Refer to Figure 30. We will show that this contradicts the third property of the set S , which states that s_{a+1} is the leftmost point on the subtrajectory $\mathcal{T}[s_{a+1}, r(s_{a+1})]$. To this end we will show that s_b is between s_{a+1} and $r(s_{a+1})$ along the trajectory \mathcal{T} , and that s_b is to the left of s_{a+1} .

Note that u occurs as a sweepline event for s_b so $s_{a+1} \prec s_b \prec u$. Therefore $s_{a+1} \prec s_b \prec u \prec$

$r(s_{a+1})$. It remains to show that s_b is to the left of s_{a+1} . Let the x -coordinate of u be x_u and consider the vertical line at x -coordinate $x_u - 1$, one unit to the left of u . Since both sweepline algorithms for s_a and s_b visited the inflection point u , we must have that the vertical line cuts $s_a s_{a+1}$ and $s_b s_{b+1}$ in such a way that s_a and s_b are to the left of the vertical line, whereas s_{a+1} and s_{b+1} are to the right of the vertical line. Therefore, s_b is to the left of s_{a+1} , completing our proof by contradiction. Hence, no inflection point u can be charged twice for the first type of sweepline event.

The second type of sweepline event is when the highest pointer p_{max} changes. Every time the second type of sweepline event occurs, there is a new upper envelope event. Therefore, the number of events of the second type is bounded by the number of upper envelope events, which by Lemma 24 is at most $O(n2^{\alpha(n)})$. Therefore, the number of sweepline events is dominated by the first type.

The total running time of the sweepline algorithm is $O(\log n)$ time per sweepline event, which leads to $O(n\alpha(n)\log^2 n)$ time in total. Therefore, the overall running time of this algorithm is $O(n\alpha(n)\log^2 n)$. \square

5.4.5 Special configuration events

We start by proving useful properties of consecutive vertices of \mathcal{T}_2 .

Lemma 26. *Let s_i and s_{i+1} be a pair of consecutive vertices of \mathcal{T}_2 . For all points $p \in \mathcal{T}[s_i, s_{i+1}]$, their set of reaches lie on a single edge e of \mathcal{T} , i.e. $\{r(p) \mid p \in \mathcal{T}[s_i, s_{i+1}]\} \subseteq e$.*

Proof. Suppose there were a vertex v in the set $\{r(p) \mid p \in \mathcal{T}[s_i, s_{i+1}]\}$. Then the point p such that $r(p) = v$ would be a reach event, which would contradict that fact that s_i and s_{i+1} are consecutive vertices of \mathcal{T}_2 , and hence all points in $\{r(p) \mid p \in \mathcal{T}[s_i, s_{i+1}]\}$ lie on an edge of \mathcal{T} . \square

Lemma 27. *Let s_i and s_{i+1} be consecutive vertices of \mathcal{T}_2 , and for any $p \in \mathcal{T}[s_i, s_{i+1}]$ let $u(p)$ be the point on the upper envelope of $\mathcal{T}[p, r(p)]$ that is one unit to the right of p . The set of points $\{u(p) \mid p \in \mathcal{T}[s_i, s_{i+1}]\}$ lies on a single edge of \mathcal{T} .*

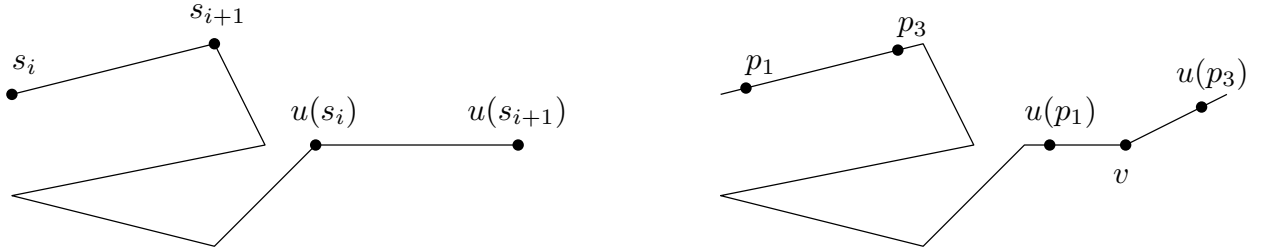


Figure 31: (Left) The consecutive vertices s_i and s_{i+1} , and the points $u(s_i)$ and $u(s_{i+1})$ one unit to their right. (Right) If $u(p_1)$ and $u(p_3)$ are on different edges, then p_1 and p_3 are not consecutive.

Proof. Assume for sake of contradiction that there are two points $p_1, p_3 \in \mathcal{T}[s_i, s_{i+1}]$ for which $u(p_1)$ and $u(p_3)$ lie on different edges of \mathcal{T} . See Figure 31, (right). There must be a vertex v of the upper envelope separating $u(p_1)$ and $u(p_3)$. As a result, it follows that there is a point $p_2 \in \mathcal{T}[p_1, p_3]$ for which $u(p_2) = v$. But now p_2 is a vertex of \mathcal{T}_2 . This contradicts the fact that p_1 and p_3 are consecutive. Therefore, all $u(p)$ for $p \in \mathcal{T}[s_1, s_2]$ lie on a single edge of \mathcal{T} . \square

Lemma 28. *Given a trajectory with n vertices, there are at most $O(n2^{\alpha(n)})$ special configuration events.*

Proof. We show the bound by showing that between any two elements of \mathcal{T}_2 , there is either a unique special configuration event, or if there are multiple they are equivalent and we need only compute one of them. We show this by using Lemmas 26 and 27 of the trajectory \mathcal{T}_2 . We require a rotated version of Lemma 27 to hold for the left cardinal direction as well as the upward cardinal direction to bound the number of occurrences of special configuration 3. Now we consider three cases.

Special Configuration 1. We use Lemma 26 of \mathcal{T}_2 to bound the number of special configuration events. We show that between consecutive events s_i and s_{i+1} , there is either a unique instance of special configuration 1, or there are multiple instances of special configuration 1 which are all equivalent and we only need to compute one of them.

Let e_p be the edge of \mathcal{T} containing p and let e_q be the edge containing q . The segment $s_i s_{i+1}$ is a subset of e_p , and by Lemma 26 of \mathcal{T}_2 , the set of reaches $\{r(p) : p \in \mathcal{T}[s_i, s_{i+1}]\}$ is a subset of e_q . Special configuration 1 states that the top-right corner of \mathcal{H}_1 lies on e_p and the bottom-left corner of \mathcal{H}_1 lies on e_q .

Let $p(t)$ be a function that slides the starting point p from s_i to s_{i+1} . Formally, let $p : [0, 1] \rightarrow \mathcal{T}[s_i, s_{i+1}]$ be a linear function so that $p(0) = s_i$ and $p(1) = s_{i+1}$. Let $\mathcal{H}(t)$ be the unit sized square with its top-right corner at $p(t) \in e_p$. See Figure 32. If $p(t)$ is in special configuration 1, then $\mathcal{H}(t)$ would also have its bottom-left corner on e_q .

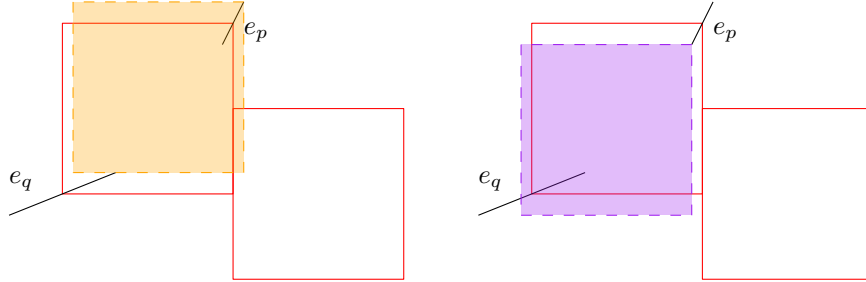


Figure 32: The square $\mathcal{H}(t)$ with top-right corner $p(t)$ on segment e_p .

There are two cases. In the first case, e_p and e_q are not parallel. Then since $\mathcal{H}(t)$ moves parallel to $p(t) = e_p$, the bottom-left corner of $\mathcal{H}(t)$ moves parallel to e_p with time. Therefore, the bottom-left corner of $\mathcal{H}(t)$ can only intersect e_q once, and we have that between s_i and s_{i+1} there is a unique instance of special configuration 1.

Otherwise, e_p and e_q are parallel. Therefore, if it is true that $\mathcal{H}(t)$ has its bottom-left corner on e_q for some value of t , then it is true for all values of $t \in [0, 1]$. Moreover, $p(t)$ and $r(p(t))$ move along e_p and e_q at the same rate since they are opposite corners of a fixed sized square. We can deduce that $\mathcal{T}[p(t), r(p(t))]$ have the same length for all $t \in [0, 1]$, in which case we only need to compute one such $p(t)$.

Special Configuration 2. We use Lemma 27 of \mathcal{T}_2 to show that it suffices to consider a unique instance of special configuration 2 between s_i and s_{i+1} . Let e_p be the segment of \mathcal{T} containing p and passing through the top-left corner of \mathcal{H}_1 . Let e_b be the segment of \mathcal{T} that passes through the bottom-right corner of \mathcal{H}_1 .

The segment $s_i s_{i+1}$ is a subset of e_p . By Lemma 27, the set of points $\{u(p) : p \in \mathcal{T}[s_i, s_{i+1}]\}$ is a subset of e_b . Let $p : [0, 1] \rightarrow \mathcal{T}[s_i, s_{i+1}]$ be a linear function so that $p(0) = s_i$ and $p(1) = s_{i+1}$. Let $\mathcal{H}(t)$ be the unit sized square with its top-left corner at $p(t) \in e_p$. See Figure 33.

If $p(t)$ were a special configuration event, then the bottom-right corner of $\mathcal{H}(t)$ is required to be on e_b . By the same reasoning as in special configuration 1, if e_p and e_b are not parallel, then there is at most one value of t where this can hold. If e_p and e_b are parallel, then computing any

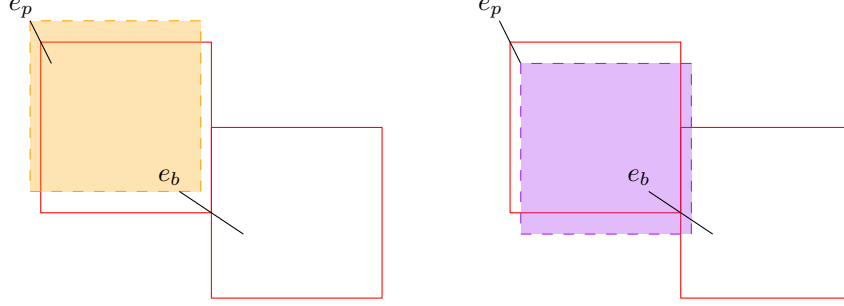


Figure 33: The square $\mathcal{H}(t)$ with top-left corner $p(t)$ on the segment e_p .

candidate would suffice. Hence it suffices to consider a unique instance of special configuration 2 between s_i and s_{i+1} .

Special Configuration 3. We use Lemmas 26 and 27 of \mathcal{T}_2 to show that it suffices to consider a unique instance of special configuration 3 between s_i and s_{i+1} . We use the Lemma 27 for both the upward and leftward cardinal directions.

Let e_p be the segment of \mathcal{T} that contains p and passes through the top-left corner of \mathcal{H}_1 . Let e_q be the segment of \mathcal{T} that contains q and passes through the bottom-right corner of \mathcal{H}_2 . Of the two distinct intersections of \mathcal{H}_1 and \mathcal{H}_2 , let e_{b_1} be the segment of \mathcal{T} that passes through the intersection of the left edge of \mathcal{H}_1 with the top edge of \mathcal{H}_2 , and let e_{b_2} be the segment of \mathcal{T} that passes through the intersection of the bottom edge of \mathcal{H}_1 with the left edge of \mathcal{H}_2 . See Figure 34.

Note that $s_i s_{i+1}$ is a subset of e_p . By Lemma 26, $\{r(p) : p \in \mathcal{T}[s_i, s_{i+1}]\}$ is a subset of e_q . By Lemma 27 in the upward direction, $\{u(p) : p \in \mathcal{T}[s_i, s_{i+1}]\}$ is a subset of e_{b_1} . If $l(p)$ is the point one unit below p on the left envelope of $\mathcal{T}[p, r(p)]$, then by Lemma 27 in the left direction, $\{l(p) : p \in \mathcal{T}[s_i, s_{i+1}]\}$ is a subset of e_{b_2} .

Now let $p : [0, 1] \rightarrow \mathcal{T}[s_i, s_{i+1}]$ be a linear function so that $p(0) = s_i$ and $p(1) = s_{i+1}$. Let $\mathcal{H}_1(t)$ be the unit sized square with its top-left corner at $p(t) \in e_p$. By the definition of an upper envelope event, $u(p(t))$ is one unit to the right of $p(t)$, and therefore $u(p(t))$ is the intersection of the right edge of $\mathcal{H}_1(t)$ and e_{b_1} . Similarly, $l(p(t))$ is the intersection of the bottom edge of $\mathcal{H}_1(t)$ and e_{b_2} .

If $p(t)$ were a special configuration event, then there would exist a square \mathcal{H}_2 so that $u(p(t))$ is on the top edge of \mathcal{H}_2 , $l(p(t))$ is on the left edge of \mathcal{H}_2 , and $r(p(t))$ is in the bottom right corner of \mathcal{H}_2 . Define $\mathcal{H}_2(t)$ to be the square with $u(p(t))$ on its top edge and $l(p(t))$ on its left edge. Then as t varies linearly, $\mathcal{H}_1(t)$ moves linearly in the plane and therefore $u(p(t))$ and $l(p(t))$ move linearly along the segments e_{b_1} and e_{b_2} . See Figure 34. Therefore, $\mathcal{H}_2(t)$ moves linearly in the plane. For the same reason as in special configuration 1 and 2, it suffices to consider a unique position where the bottom-right corner of $\mathcal{H}_2(t)$ is on the segment e_q .

Summary. In all special configurations there is a constant number of events between any two vertices of \mathcal{T}_2 . Therefore, the number of vertices of \mathcal{T}_2 is an upper bound on the number of special configuration events up to a constant factor. By

Lemma 24, the number of vertices of \mathcal{T}_2 is at most $O(n2^{\alpha(n)})$, so there are at most $O(n2^{\alpha(n)})$ special configuration events in total. \square

Lemma 29. *Given a trajectory with n vertices, one can compute all special configuration events in $O(n2^{\alpha(n)} \log^2 n)$ time.*

Proof. We use the same notation as in the proof of Lemma 28. We compute the set \mathcal{T}_2 . We take a pair of consecutive elements s_i and s_{i+1} . We compute the segment e_p that contains $\mathcal{T}[s_i, s_{i+1}]$. We use the reach data structure from Lemma 18 to compute the reach of p and therefore compute the

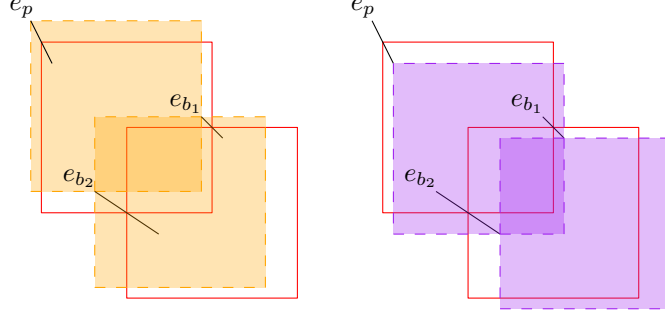


Figure 34: Sliding \mathcal{H}_1 and \mathcal{H}_2 along e_p , e_{b_1} and e_{b_2} .

segment e_q . We use the upper envelope data structure in Tool 2 to query e_b (or both e_{b_1} and e_{b_2}). We let $p : [0, 1] \rightarrow e_p$ be the linear function defined in the proof of Lemma 28.

If we are in special configuration 1 or 2, we check if the translation is parallel to e_q or e_b respectively, in which case we return the first point of $\mathcal{T}[s_i, s_{i+1}]$. Otherwise, we compute the function $\mathcal{H}(t)$ of squares parametrised by t . The square $\mathcal{H}(t)$ has its top-right, or top-left corner at $p(t)$ for special configurations 1 and 2 respectively. Then we track the segment formed by the bottom-right corner of $\mathcal{H}(t)$ as we vary t . We return the value of t where the bottom-right corner of $\mathcal{H}(t)$ lies on e_q .

If we are in special configuration 3, we compute the function $\mathcal{H}_1(t)$ of a square with its top-right corner on $p(t)$. Then we compute the intersections $u(p(t))$ and $l(p(t))$ of $\mathcal{H}_1(t)$ with e_{b_1} and e_{b_2} respectively. We let $\mathcal{H}_2(t)$ be the square with its top edge of $u(p(t))$ and its left edge of $l(p(t))$. We track the segment formed by the bottom-right corner of $\mathcal{H}_2(t)$ as we vary t . We return the value of t where the bottom-right corner of $\mathcal{H}_2(t)$ lies on e_q .

Now we analyse the running time of this algorithm. Building Tool 2 takes $O(n\alpha(n) \log n)$ time. This is dominated by the $O(n\alpha(n) \log^2 n)$ time it takes to compute \mathcal{T}_2 (Corollary 1 and Lemma 24). Between each pair (s_i, s_{i+1}) , we query the reach data structure and the upper envelope data structure, which takes $O(\log^2 n)$ and $O(\log n)$ time respectively. Constructing the functions $p(t)$, $\mathcal{H}_1(t)$, $u(p(t))$, $l(p(t))$ and $\mathcal{H}_2(t)$ are constant sized problems and only takes constant time. Therefore, the time to compute \mathcal{T}_2 is $O(n\alpha(n) \log^2 n)$ we spend $O(\log^2 n)$ query time for each element of \mathcal{T}_2 . Since the size of \mathcal{T}_2 is $O(n2^{\alpha(n)})$ by

Lemma 28, the total running time of this algorithm is $O(n2^{\alpha(n)} \log^2 n)$. \square

5.5 Summary

We summarise the results of Sections 5.4.1-5.4.5 in the table below. Putting it all together, we obtain Theorem 8.

	#events	computation time
Vertex events	$O(n)$	$O(n)$
Reach events	$O(n)$	$O(n \log^2 n)$
Bounding box events	$O(n)$	$O(n \log^2 n)$
Bridge events	$O(n)$	$O(n \log^2 n)$
Upper envelope events	$O(n2^{\alpha(n)})$	$O(n\alpha(n) \log^2 n)$
Special configuration events	$O(n2^{\alpha(n)})$	$O(n2^{\alpha(n)} \log^2 n)$.

Theorem 8. *The trajectory \mathcal{T}_3 has $O(n2^{\alpha(n)})$ vertices, and can be constructed in time $O(n2^{\alpha(n)} \log^2 n)$.*

5.6 Computing the optimal subtrajectory

By Theorem 7 there is a longest 2-coverable trajectory that starts at a point $p \in S$. By Theorem 8 this set S has size $m = O(n2^{\alpha(n)})$ and we can compute it in $O(n2^{\alpha(n)} \log^2 n)$ time. Using Corollary 1 we can compute a longest 2-coverable subtrajectory starting at each point in S in $O(n \log n + m \log^2 n) = O(n2^{\alpha(n)} \log^2 n)$ time. We therefore obtain the following result:

Theorem 9. *Given a trajectory \mathcal{T} with n vertices, there is an $O(n2^{\alpha(n)} \log^2 n)$ time algorithm to compute a longest 2-coverable subtrajectory of \mathcal{T} .*

6 Concluding Remarks

We presented algorithms to decide if a set of segments is k -coverable for $k = 3, 4$, data structures for answering if subtrajectories are k -coverable for $k = 2, 3$, and algorithms to compute the longest k -coverable subtrajectory for $k = 1, 2$. One open problem is whether we can extend our algorithms to larger values of k . Another open problem is whether we can improve the bounds on the number of starting points of the longest 2-coverable subtrajectory, and whether we can compute them more efficiently.

References

- [1] Pankaj K. Agarwal and Cecilia Magdalena Procopiuc. Exact and approximation algorithms for clustering. *Algorithmica*, 33(2):201–226, 2002.
- [2] Michael A. Bender and Martin Farach-Colton. The LCA problem revisited. In *Proceedings of the 4th Latin American Symposium on Theoretical Informatics*, volume 1776 of *Lecture Notes in Computer Science*, pages 88–94. Springer, 2000.
- [3] Sergey Bereg, Binay Bhattacharya, Sandip Das, Tsunehiko Kameda, Priya Ranjan Sinha Mahapatra, and Zhao Song. Optimizing squares covering a set of points. *Theoretical Computer Science*, 729:68–83, 2018.
- [4] Bernard Chazelle and Leonidas J. Guibas. Fractional cascading: I. A data structuring technique. *Algorithmica*, 1(2):133–162, 1986.
- [5] Maria Luisa Damiani, Hamza Issa, and Francesca Cagnacci. Extracting stay regions with uncertain boundaries from GPS trajectories: A case study in animal ecology. In *Proceedings of the 22nd ACM SIGSPATIAL International Conference on Advances in Geographic Information Systems*, pages 253–262, 2014.
- [6] Zvi Drezner. On the rectangular p -center problem. *Naval Research Logistics*, 34(2):229–234, 1987.
- [7] Robert J. Fowler, Mike Paterson, and Steven L. Tanimoto. Optimal packing and covering in the plane are NP-complete. *Information Processing Letters*, 12(3):133–137, 1981.
- [8] Joachim Gudmundsson and Michael Horton. Spatio-temporal analysis of team sports. *ACM Computing Surveys*, 50(2):22, 2017.
- [9] Joachim Gudmundsson, Marc van Kreveld, and Frank Staals. Algorithms for hotspot computation on trajectory data. In *Proceedings of the 21st ACM SIGSPATIAL International Conference on Advances in Geographic Information Systems*, pages 134–143, 2013.

- [10] John Hershberger. Finding the upper envelope of n line segments in $O(n \log n)$ time. *Information Processing Letters*, 33(4):169–174, 1989.
- [11] Michael Hoffmann. Covering polygons with few rectangles. In *Abstracts 17th European Workshop Computational Geometry*, pages 39–42, 2001.
- [12] Ruei-Zong Hwang, Richard C. T. Lee, and Ruei-Chuan Chang. The slab dividing approach to solve the Euclidean p -center problem. *Algorithmica*, 9(1):1–22, 1993.
- [13] Priya Ranjan Sinha Mahapatra, Partha P. Goswami, and Sandip Das. Maximal covering by two isothetic unit squares. In *Canadian Conference on Computational Geometry*, pages 103–106, 2008.
- [14] Nimrod Megiddo. Applying parallel computation algorithms in the design of serial algorithms. In *22nd Annual Symposium on Foundations of Computer Science*, pages 399–408. IEEE, 1981.
- [15] Nimrod Megiddo and Kenneth J. Supowit. On the complexity of some common geometric location problems. *SIAM Journal of Computing*, 13(1):182–196, 1984.
- [16] Doron Nussbaum. Rectilinear p -piercing problems. In *Proceedings of the 1997 International Symposium on Symbolic and Algebraic Computation*, pages 316–323, 1997.
- [17] Sanjib Sadhu, Sasanka Roy, Subhas C. Nandy, and Suchismita Roy. Linear time algorithm to cover and hit a set of line segments optimally by two axis-parallel squares. *Theoretical Computer Science*, 769:63–74, 2019.
- [18] Michael Segal. On piercing sets of axis-parallel rectangles and rings. *International Journal of Computational Geometry and Applications*, 9(3):219–234, 1999.
- [19] Micha Sharir and Pankaj K. Agarwal. *Davenport-Schinzel sequences and their geometric applications*. Cambridge University Press, 1995.
- [20] Micha Sharir and Emo Welzl. Rectilinear and polygonal p -piercing and p -center problems. In *Proceedings of the 12th Annual Symposium on Computational Geometry*, pages 122–132, 1996.
- [21] Andreas Stohl. Computation, accuracy and applications of trajectories—A review and bibliography. *Developments in Environmental Science*, 1:615–654, 2002.